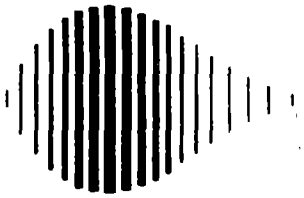

NATIONAL CENTER FOR EARTHQUAKE ENGINEERING RESEARCH
State University of New York at Buffalo

SEISMIC DAMAGE ASSESSMENT OF REINFORCED CONCRETE MEMBERS

by

Y. S. Chung, C. Meyer, and M. Shinozuka
Department of Civil Engineering and
Engineering Mechanics
Columbia University
New York, NY 10027-6699

Technical Report NCEER-87-0022

October 9, 1987

This research was conducted at Columbia University and was partially supported by the National Science Foundation under Grant No. ECE 86-07591

NOTICE

This report was prepared by Columbia University as a result of research sponsored by the National Center for Earthquake Engineering Research (NCEER). Neither NCEER, associates of NCEER, its sponsors, Columbia University, nor any person acting on their behalf:

a. makes any warranty, express or implied, with respect to the use of any information, apparatus, method, or process disclosed in this report or that such use may not infringe upon privately owned rights; or

b. assumes any liabilities of whatsoever kind with respect to the use of, or for damages resulting from the use of, any information, apparatus, method or process disclosed in this report.

SEISMIC DAMAGE ASSESSMENT OF REINFORCED CONCRETE MEMBERS

by

Y.S. Chung[1], C. Meyer[2] and M. Shinozuka[3]

October 9, 1987

Technical Report NCEER-87-0022

NCEER Contract Number 86-3033

NSF Master Contract Number ECE-86-07591

1 Graduate Research Assistant, Dept. of Civil Engineering and Engineering Mechanics, Columbia University
2 Associate Professor, Dept. of Civil Engineering and Engineering Mechanics, Columbia University
3 Renwick Professor, Dept. of Civil Engineering and Engineering Mechanics, Columbia University

NATIONAL CENTER FOR EARTHQUAKE ENGINEERING RESEARCH
State University of New York at Buffalo
Red Jacket Quadrangle, Buffalo, NY 14261

ABSTRACT

This report starts with a fundamental discussion of damage, which reinforced concrete members sustain under large inelastic cyclic loads similar to those experienced during a severe earthquake. A large number of damage indices, which have been proposed in the literature, are discussed and critically evaluated under the criterion of usefulness for structural analysis and seismic risk assessment.

A new damage index is presented, which the authors believe is a rational measure of the physical response characteristics of reinforced concrete members and better suited for nonlinear structural analysis than those that have been proposed previously. Unfortunately, experimental data, on which the calibration of the new model depends, are scarce, therefore it is recommended that systematic low-cycle fatigue tests be undertaken to strengthen the theoretical basis for the model.

TABLE OF CONTENTS

TABLE OF CONTENTS (Continued)

LIST OF FIGURES

LIST OF FIGURES (Continued)

LIST OF TABLES

Acknowledgements

This research was supported in part by the National Center of Earthquake Engineering Research, under Grant No. SUNYRF NCEER-86-3033. The support is gratefully acknowledged.

We would like to thank Professor Mizuhata of Kobe University in Japan and Professor Park of SUNY at Buffalo, New York for providing detailed information about their respective damage models.

1. Introduction

Current aseismic design philosophy for reinforced concrete structures relies strongly on energy dissipation through large inelastic deformations. As a result, structural members resisting the lateral loads of catastrophic earthquakes such as the recent 1985 Mexico City earthquake, will undergo large cyclic inelastic deformations. These cause a certain amount of damage in the form of large cracks and, in particularly severe cases, can lead to structural collapse. In the design of reinforced concrete structures against earthquakes, the concepts of damage and damageability thus play a central role. The economy of construction requires that the accepted level of damage be tied to the expected risk of earthquake exposure. Thus, for minor earthquakes of relatively frequent occurrence, no damage except possibly that of minor cosmetic nature is acceptable. For medium earthquakes with considerably larger return intervals, some damage of nonstructural components is generally considered to be acceptable. For example, the Union Bank Building in downtown Los Angeles suffered such damage during the 1971 San Fernando earthquake, in the form of broken bathroom tiles and cracked plaster, the repair of which cost less than one year's earthquake insurance premium. For catastrophic earthquakes of very low probability of occurrence, a considerable amount of damage is acceptable. But this should be repairable, and the prevention of collapse should be the supreme design objective at any time.

This staggered design philosophy places a considerable demand on the engineer's ability to analyze the nonlinear response of reinforced concrete structures subjected to strong seismic loads. It requires tools to predict the level of damage as a function of intensity of earthquake exposure and, with this, the following two separate tasks: First, it is necessary to introduce a reliable and useful definition of damage. Second, a mathematical model is required which can simulate the nonlin-

ear response of reinforced concrete members with sufficient accuracy. With these tools in hand, it will be possible to make rational predictions of the reliability of reinforced concrete buildings in seismic environments.

This report addresses the first task in form of a fundamental discussion of damage and the definition of a damage index that is essential for the successful completion of the second task. Based on the experience from past strong earthquakes and laboratory investigations, damage of reinforced concrete structures is the result of a combination of level of exposure and the number of exposures or load cycles, a phenomenon generally known as low-cycle fatigue. Thus, a ductility ratio as a sole measure of damage is not sufficient as a damage indicator for our purposes. The number of cycles, or rather the dissipated energy has to be taken into account as well. A logical approach would be to establish, similar to common fatigue life predictions, a relationship between constant stress or strain amplitude and the number of cycles to failure. Variations in load amplitude encountered in real life situations are then accounted for by a rule such as Miner's hypothesis. This approach has proven successful if applied to metal structures. Reinforced concrete, however, is a much more complicated material, which cannot be described by comparably simple equations as metals do. The heterogeneity of concrete plus the complex interactions between reinforcing steel and concrete cause complicated modifications of the load level, number of cycles to failure and their relationship, which may be simulated with appropriate damage acceleration factors.

The next chapter will present a fundamental discussion of damage and its ramifications for nonlinear structural analysis. Since most damage indices are normalized to reach a value of unity for damage levels tantamount to failure, this discussion will have to include also the definition of failure. In Chapter 3, the various damage indices which have been proposed in the past, will be discussed and critically eval-

uated under the criterion of usefulness for structural analysis and seismic reliability analysis. In Chapter 4, a new damage index will be presented, which the authors believe is a rational measure of the physical response characteristics of reinforced concrete members and is better suited for nonlinear structural analysis than those that have been proposed previously. Final conclusions and recommendations for further study will be given in Chapter 5.

2. Fundamental Discussion of Failure and Damage of RC Members

Any attempt of devising mathematical models to quantify damage in a rational way should set out with a clear and precise definition of damage. This requirement is all the more essential, because "damage" is a widely used word, that is used to describe all kinds of different phenomena and is prone to subjective interpretation. In the context of our discussion, damage of a RC member shall be defined to signify a certain degree of physical deterioration with precisely defined consequences regarding the member's capacity to resist further load. Similarly, by "failure" of a member is meant a specific level of damage, which is equivalent to a certain amount of residual capacity to resist further load. In contrast to metal structures, failure can seldom be defined in an objectively unique way. It typically is taken to be a rather arbitrarily determined damage level with a corresponding low level of residual load-resisting capacity. A damage index is usually defined as the damage value normalized with respect to the failure level so that a damage index value of unity corresponds to the (arbitrarily defined) failure.

As an illustration, Fig. 2.1 shows a typical response of a reinforced concrete cantilever beam to progressively increasing load cycles. As can be clearly seen, the stiffness of the member gradually decreases, once the yield capacity of the member has been exceeded. It takes a significant increase in loading until the strength deteriorates as well, i.e. when the force necessary to cause a given tip deflection, decreases in subsequent cycles. Fig. 2.1 also demonstrates the difficulty of defining failure. According to Fig. 2.2, which shows a cantilever beam like the one of Fig. 2.1 after termination of the test, even rubble can still carry load. Thus, any failure definition has to be somewhat arbitrary. Some researchers(1,15,23) have proposed to define the failure point as the load level, at which the residual strength has been reduced to 75% of the first yield load level. Later on, we shall see that this

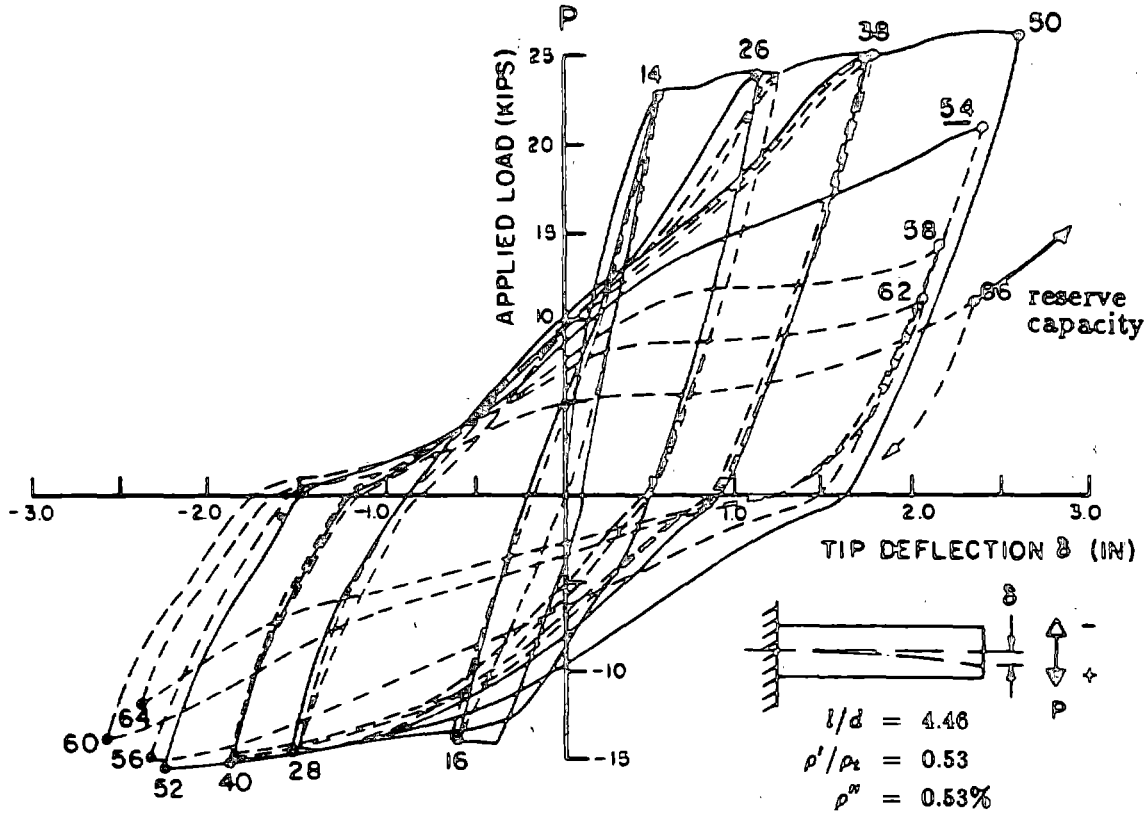

Fig. 2.1 - Typical inelastic respoinse of RC member
(Experiment by Ma, Bertero and Popov, Ref. 21)

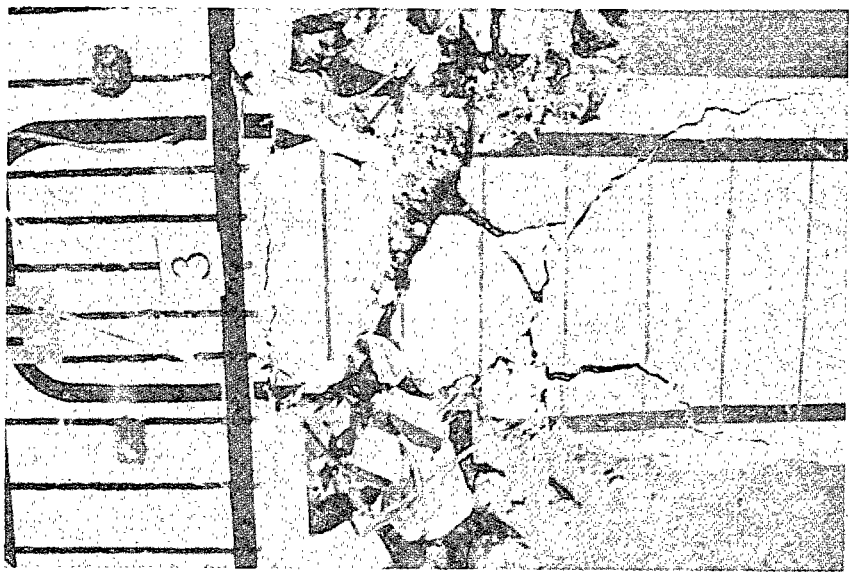

Fig. 2.2 - Specimen after determination of test
(Experimental by Hwang and Scribner, Ref. 16)

definition is still not sufficiently precise, since the apparent residual strength may increase with further displacement increase, Fig. 2.1. In Chapter 4, a procedure will be outlined by which this failure definition can be modified appropriately.

In order to understand the various factors that contribute to damage, it is necessary to study the behaviour of plain concrete at different load levels. Damage can be closely correlated to the amount of cracking (both are irreversible) and expresses itself as the degree of nonlinearity of the stress-strain diagram, Fig. 2.3. Thus, the factors that control cracking behaviour of concrete are also responsible for the afflicted damage level. For low levels of stress, up to about $0.3f_c'$ to $0.5f_c'$, only moderate amounts of microcracking can be observed so that the stress-strain response is almost linear. Beyond this stress range, microcracks propagate and coalesce into macrocracks, and the increased damage expresses itself in an accelerating increase of nonlinearity of the stress-strain curve.

It is well understood that internal flaws and cracks exist in concrete even before any loads have been applied(22). Sources of microcracking are due to segregation and bleeding, particularly beneath large aggregate particles and reinforcing bars. The most frequent microcracks, however, originate from bond cracks at the cement-aggregate interface, and are due either to differences in the elastic moduli of the cement paste and aggregate, or differences in their thermal expansion coefficients and different responses to changes in moisture content. The incompatibility of the Young's moduli may lead to considerable stress concentrations due to differential volume changes during continued cement hydration, drying of concrete, or temperature changes(22).

As concrete is subjected to stress, the stress concentrations near the microscopic flaws invariably lead to microcracks, which multiply and propagate either along the cement-aggregate interface or into the cement matrix itself as shown in Fig. 2.4. As

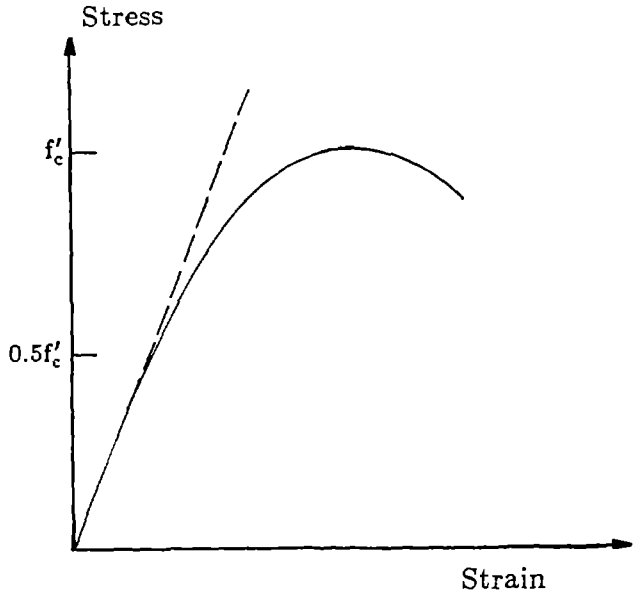

Fig. 2.3 - Typical stress-strain curve of concrete

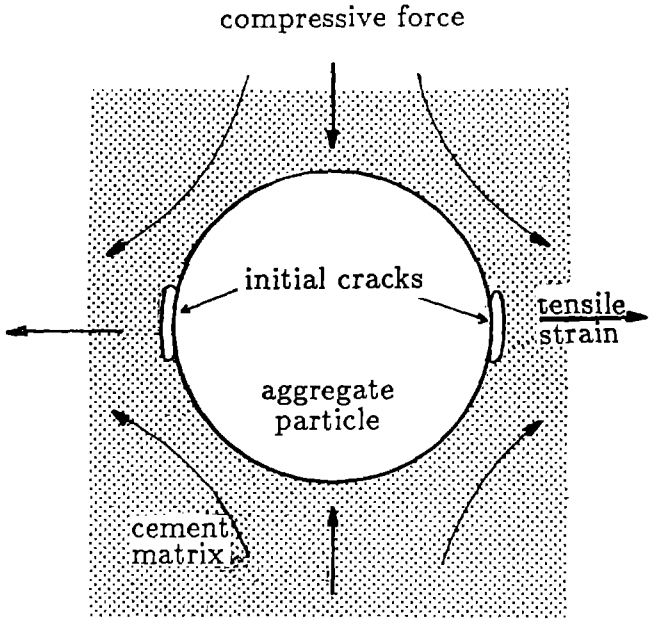

Fig. 2.4 - Crack propagation along the cement-aggregate interface(Ref. 22)

the stress level exceeds about half of the ultimate strength, a more extensive and continuous macrocrack system begins to develop, which softens the material, giving it the strongly nonlinear stress-strain relationship. Beyond approximate $0.75f_c'$, the growth rate of the macrocracks accelerates until it becomes unstable, leading to failure.

The strength of plain concrete and its damageability depend upon a large number of factors. The most important one is the water-cement ratio or, more precisely, the material density, which is a function of the water-cement ratio. Another significant influence factor is the state of stress. Under biaxial and triaxial compression, not only the material strength is increased appreciably, but also the stress-strain behaviour becomes more linear, indicating a delay of the softening crack formation and damage, Fig. 2.5. Under hydrostatic pressure, one is tempted to claim that concrete cannot fail. The corresponding stress-strain curve does indeed maintain a positive slope presumably indefintely, Fig. 2.6. In reality, however, the structure of the material does get damaged progressively with higher pressure, which manifests itself in a loss of residual uniaxial compressive strength(35). After applying a hydrostatic pressure of about $6f_c'$, a drop of 25% has been reported for the uniaxial strength f_c'(35), Fig. 2.7. When studying the response of plain concrete to cyclic loads, the most striking aspect of the material behaviour is how the material "remembers" the amount of damage sustained in all preceding load cycles. As a consequence, the cyclic stress-strain curve is neatly bounded by the monotonic stress-strain curve, Fig. 2.8(38). After one load cycle has been completed and a certain amount of damage been inflicted, the material will respond to a subsequent load cycle as if this were a continuation of the previous one, after the maximum previous load level has been reached and exceeded. Remarkable is the considerable residual strain, which is an indication of the amount of damage sustained so far.

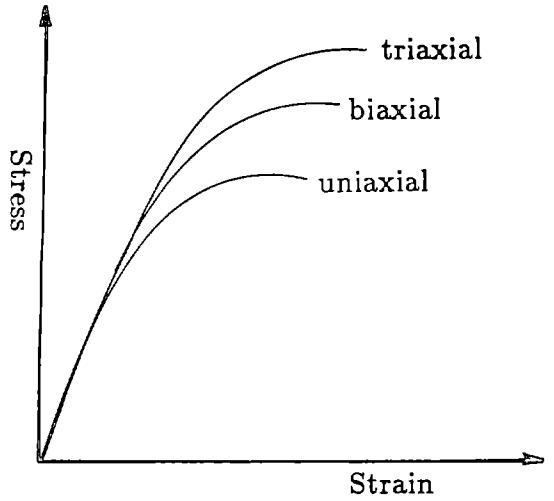

Fig. 2.5 - Typical stress-strain curves for concrete with and without confinement

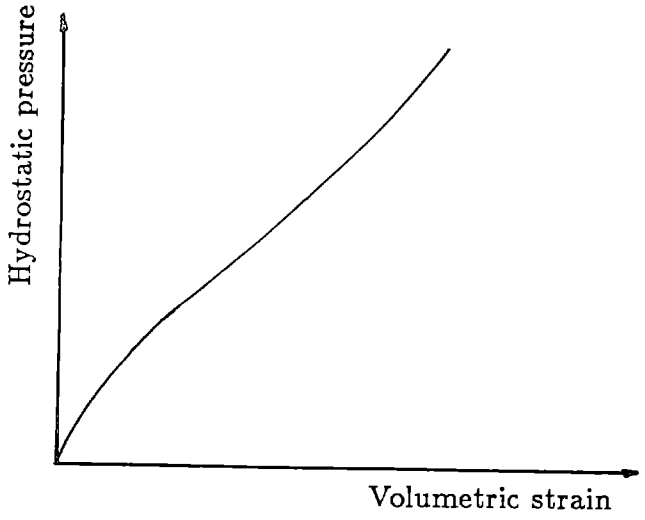

Fig. 2.6 - Hydrostatic stress-strain behaviour of concrete (Ref. 35)

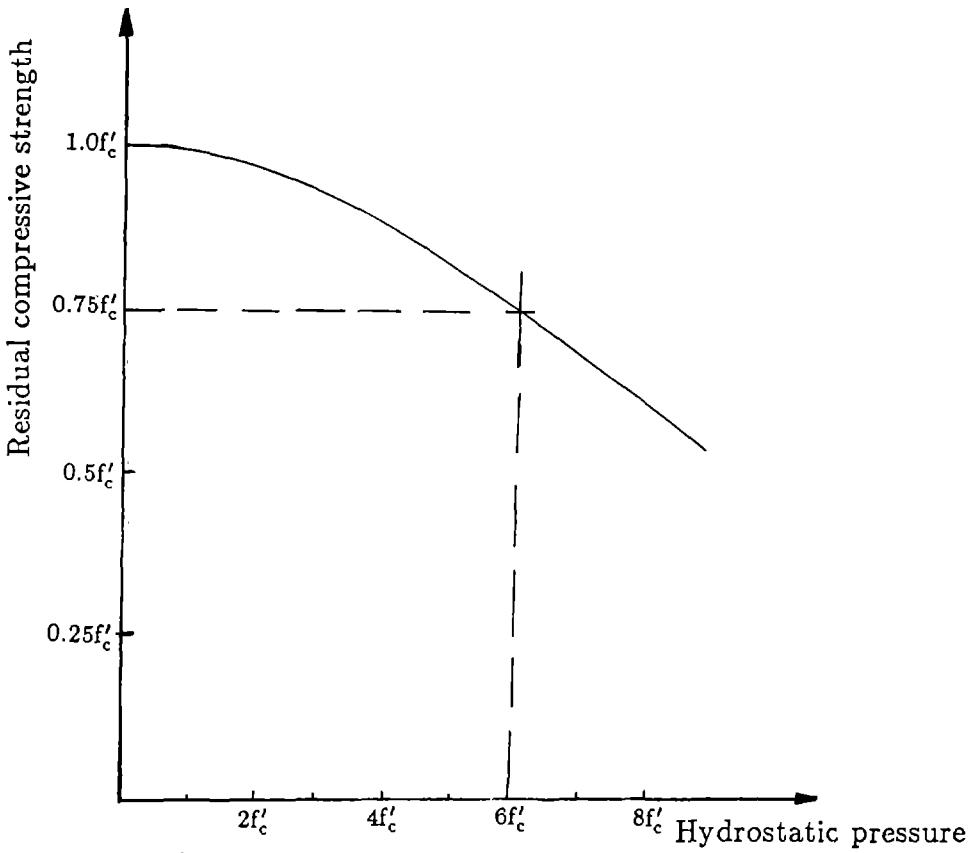

Fig. 2.7 - Residual compressive strength of concrete after application and removal of hydrostatic pressure(Ref. 35)

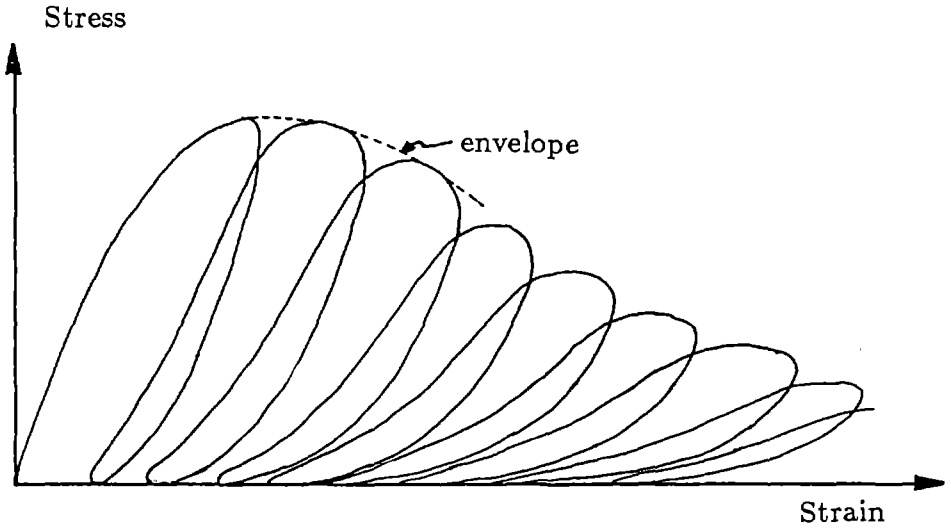

Fig. 2.8 - Cyclic stress-strain curve(Ref. 38)

The response of reinforced concrete to load is complicated by the complex interaction between steel and concrete. This is reflected in the number of possible failure modes, Fig. 2.9:

1) a flexural failure mode due to the crushing of concrete in compression after considerable yielding of tensile steel has taken place;
2) a flexural failure mode due to the fracture of tensile reinforcement following large plastic deformations of the steel;
3) a flexural failure mode due to the concrete crushing in compression before tensile steel started to yield;
4) a flexural failure mode controlled by buckling of the compression reinforcement after spalling of the concrete cover;
5) a flexure-shear failure, initiated by vertical flexural cracks, which, after load reversals, link up and cause a shear failure along virtually vertical planes, against which vertical stirrup reinforcement is basically ineffective;
6) a web-shear failure, triggered by diagonal cracks which propagate across the entire member section;
7) a web-shear failure in which the vertical stirrups yield, after diagonal cracks have opened up, and the dowel action of flexural reinforcement has spalled off the concrete cover;
8) a bond failure in which the reinforcing bars pull out from the concrete, either with or without a prior shear crack propagating along the reinforcement.

Conventional reinforced concrete design philosophy calls for such member detailing that all but the first two failure modes are precluded, to assure a truely ductile failure mode. All others are characterized by more or less sudden drops in strength, which are typical of brittle materials. For dynamically applied cyclic

loads it is difficult to predict the failure mode even for "properly" detailed members. There are two reasons for this. First, the so-called strain rate effect influences the various failure modes to different degrees. Thus, even a ductile steel member can experience a brittle fracture, because the resistance against sliding(responsible for ductile failure) increases more rapidly with increasing loading rate than the resistance to separation. The second reason is the fact that load reversals inflict different levels of damage in the various modes. Bond deterioration and shear cracking typically progress much more rapidly under cyclic loading than flexural strength degradation. As a result, reinforced concrete members subjected to earthquake-type loads are much more likely to fail in bond or shear than in flexure, even if properly designed for monotonically applied loads.

The progressive accumulation of damage in a material up to the point of failure under repeated load application has been studied extensively in metals and is generally known as "fatigue"(29,30). Also in metals, microscopically small defects, inclusions etc exist, which, upon the application of stress, are responsible for local stress concentrations and gradual propagation of cracks. After a certain number of applications of some load level S_i, these cracks will cause complete failure. This number of cycles to failure, N_i, is generally referred to as the "fatigue life", or simply "life" of the material. It signifies that each load cycle inflicts a certain amount of irreversible damage, like the passage of some time unit of the life span of the material. The relationship between stress level S_i and fatigue life N_i is plotted in a so-called S-N curve, Fig. 2.10, typically on a logarithmic scale.

If the material is subjected to a history of varying stress levels, the prediction of the fatigue life is much more difficult. In this case, it is common practice to utilize Miner's hypothesis,

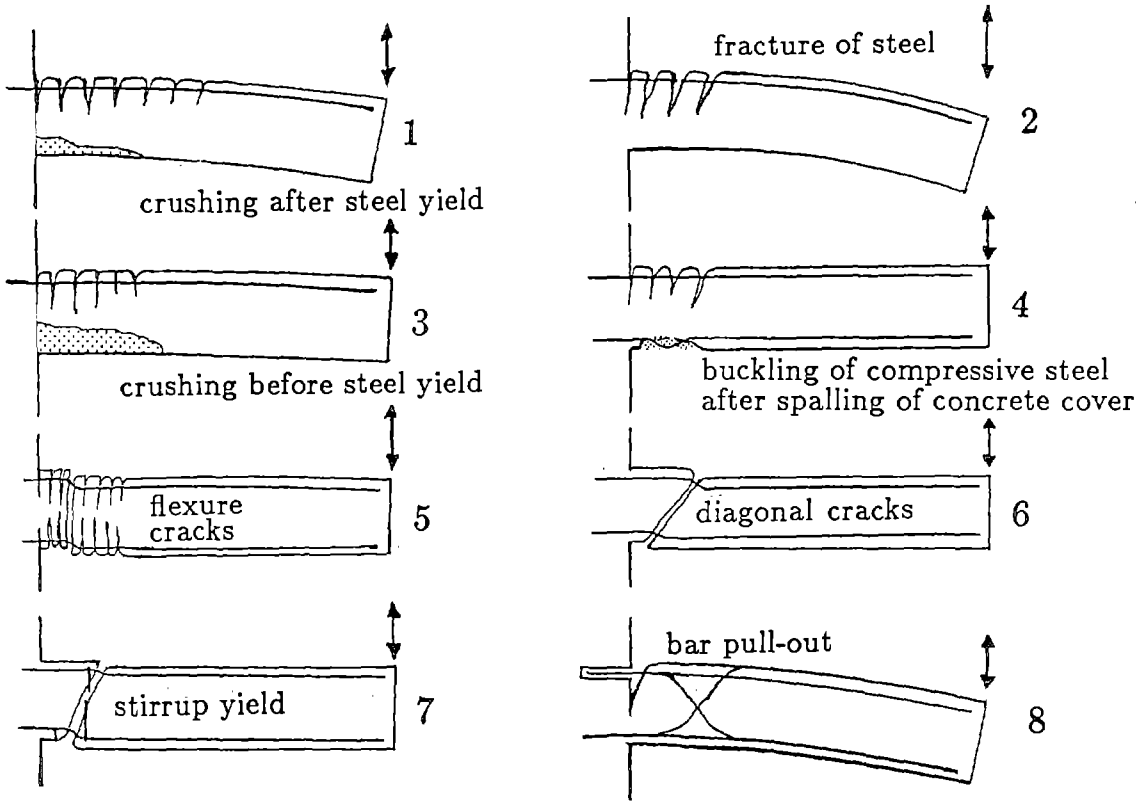

Fig. 2.9 - Possible failure modes of reinforced concrete members

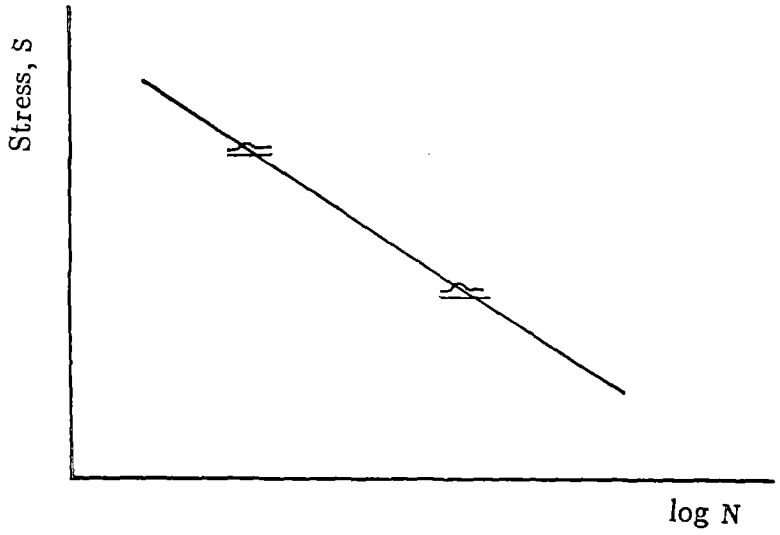

Fig. 2.10 - Typical S – N curve for metals

$$\sum_i \frac{n_i}{N_i} = 1 \qquad (2.1)$$

where

N_i : Number of cycles with stress level S_i leading to failure

n_i : number of cycles with stress level S_i actually applied

Eq (2.1) assumes that the accumulation of damage is linear and independent of the load history. Thus, the three load histories of Fig. 2.11 are assumed to result in exactly the same amount of damage in the end.

Even for metals the straight application of Miner's rule is not well supported by experimental evidence, so that so-called modified Miner's rules have been proposed(11). As we shall see, there is even less justification to apply Miner's rule in the form of Eq (2.1) to reinforced concrete.

The study of low-cycle fatigue of reinforced concrete is handicapped by a dearth of experimental data. To begin with, instead of deriving S-N curves, it has been common to replace the number of cycles by the energy dissipated, whereby this energy is typically normalized with regard to the energy stored when the member is stressed up to the yield level, Fig. 2.12. If the member were not to degrade under large inelastic load cycles, the dissipated energy index E_i would be exactly proportional to the number of applied load cycles. In reality, however, the amount of energy dissipated in each load cycle decreases with progressive damage, until some failure level has been reached. Even then, in analogy to an S-N curve, given the necessary experimental data, it is possible to present the relationship between deformation level D_i and the total energy dissipation capacity.

As was pointed out, the number of cycles to failure and total energy dissipation capacity are not corresponding one-to-one. In an S-N relationship, N_i is a truely

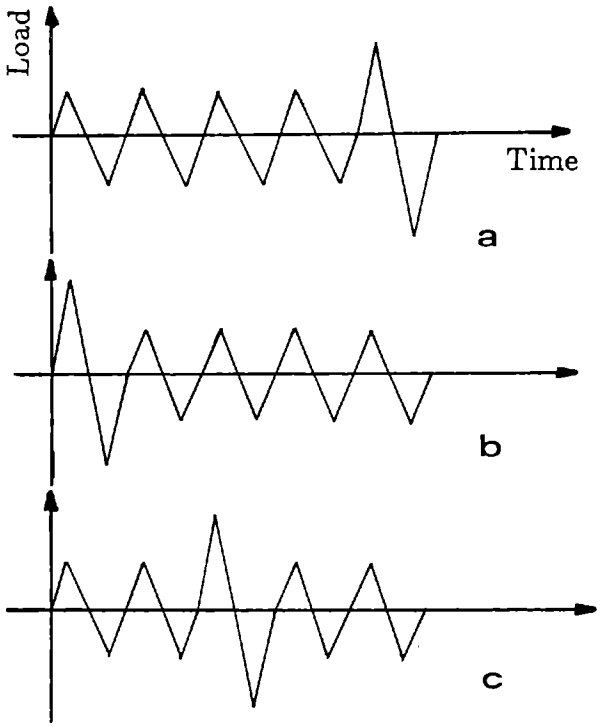

Fig. 2.11 - Three different load histories

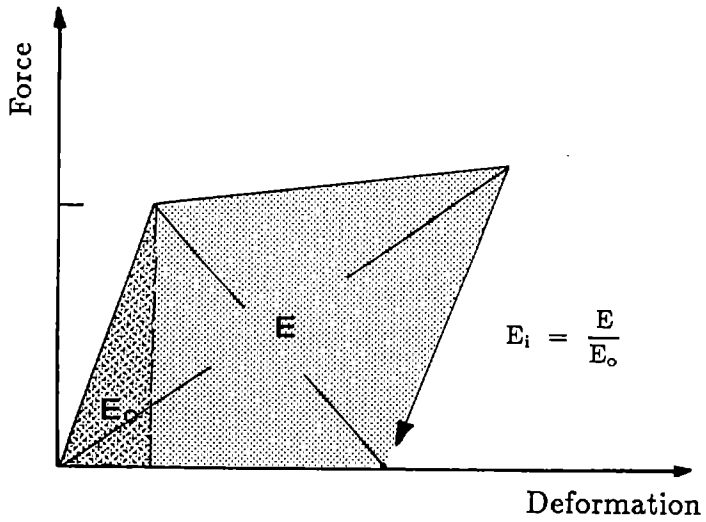

Fig. 2.12 - Typical definition of normalized energy

independent variable, which can be determined experimentally for a given stress level S_i. The energy dissipated in a single load cycle, on the other hand, is not independent of the deformation level. In fact, if the deformation level were to be chosen arbitrarily low so that the load-deformation relationship would remain linear, no energy would be dissipated at all. Thus, based on this argument and experimental evidence, a $D_i - E_i$ curve has to have a shape as shown in Fig. 2.13, which shows that there exists a certain range of load amplitudes for which a RC member will dissipate a maximum amount of energy.

The energy dissipation capacity of a reinforced concrete member is dependent on a number of variables:

1) the amount of confinement reinforcement;
2) the strength of concrete;
3) the amount of longitudinal reinforcement;
4) member detailing such as sufficient anchorage of reinforcement;
5) the amount and arrangement of shear reinforcement;
6) the load history;
7) the moment-to-shear ratio or shear span;
8) the magnitude of axial force.

In particular, it can be observed from some laboratory experiments(15) that the failure mode is closely related to the formation of initial cracks that eventually may become critical. Consider the first two load histories schematically shown in Fig. 2.11. Assume that the four low level load cycles of Fig. 2.11a cause a certain amount of damage associated with a specific kind of cracking. The energy absorption capacity will be almost intact before the member is subjected to the critical fifth load cycle. The damage caused by this final load cycle is not only much more severe, but also the associated cracking may predispose the member to

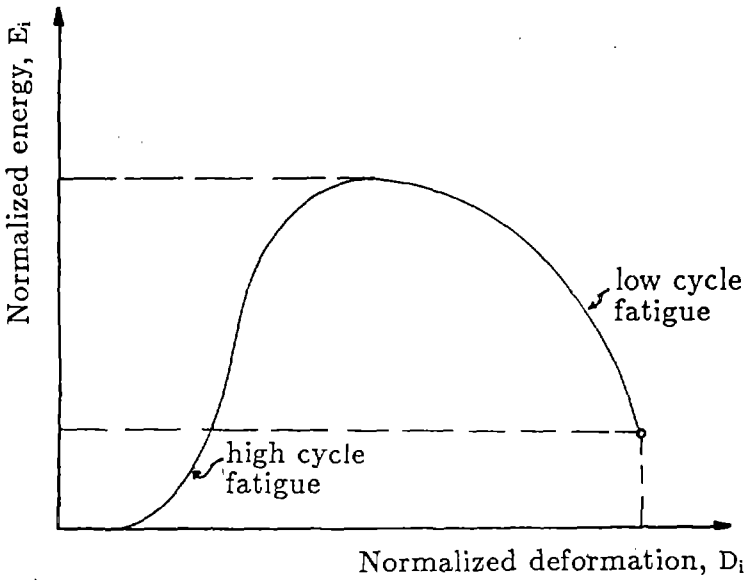

Fig. 2.13 - $E_i - D_i$ curve for reinforced concrete member

a different failure mode. If the member were subjected to the load history of Fig. 2.11b, it is possible that the response and energy absorption capacity are completely different. This would be the case if the initial critical load cycle severely damages the member, drastically reducing its residual strength and energy absorption capacity. In this case, the member may not be able to sustain the remaining four low level load cycles. Thus, it is likely that not only the total energy dissipation capacity of a RC member is dependent on the load history, but its failure mode as well.

A rational scheme will have to be developed that recognizes the physical characteristics of the material and thus is capable of predicting the remaining energy dissipation capacity or life of a member. It is this reserve capacity and residual strength that determine the reliability of a member and its chances of survival if subjected to further severe cyclic load.

In the following chapter, most pertinent damage models that have been proposed in the past will be discussed and critically assessed in view of what we know about the physical aspects of damage.

3. Critical Assessment of Previous Damage Models

In this chapter we shall review most of the damage models that have been proposed so far to characterize structures subjected to strong seismic motions. This discussion must also include the various energy indices which closely relate to damage measures for RC members. All of these are categorized into four groups: damage indices proposed primarily for structural steel components, empirical damage definitions, normalized dissipated energy indices, and damage indices developed for reinforced concrete structures on the basis of theoretical principles.

3.1 Damage Indices for Structural Steel Components

The behaviour of a composite material such as reinforced concrete is considerably different from that of a homogeneous material such as steel. It is therefore unlikely that damage models proposed for structural steel are directly applicable to reinforced concrete. Some of these models, however, can form the basis for RC damage models, provided some important parameters are modified appropriately. In the following, three damage models shall be mentioned, which had been developed to describe low-cycle fatigue behaviour of structural steel.

3.1.1 Yao and Munse(1962)

For low-cycle fatigue of metal structures during strong earthquakes, Yao and Munse (48) presented a general hypothesis which relates the cumulative effect of plastic strain to the low-cycle fatigue behaviour. If the time history of plastic strain in the extreme fibre of the critical strain section is known, the damage factor, D^i, resulting from the i-th cycle of plastic strain, from compression to tension, Fig. 3.1, can be found as:

$$D^i = \left(\frac{\Delta_i}{\Delta u_i}\right)^{\alpha_i} \tag{3.1}$$

where

Δ_i : incremental positive plastic strain during the i – th cycle

Δu_i : tension plastic strain to cause failure during the i – th cycle

$\alpha_i = 1 - 0.86\left(\frac{\Delta_i'}{\Delta_i}\right)$; fatigue damage exponent

$\frac{\Delta_i'}{\Delta_i}$: relative plastic strain ratio as shown in Fig.3.1

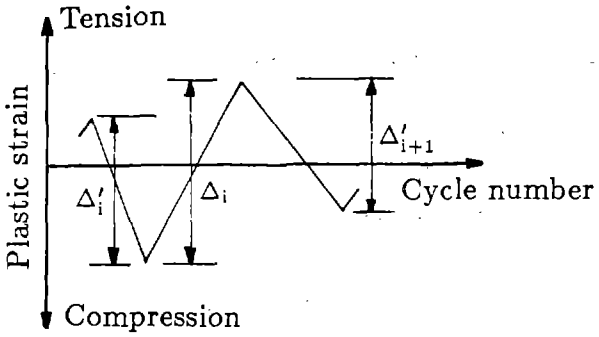

Fig. 3.1 - Typical response cycle for metals(Ref. 17)

The damage of the member due to "n" cycles of straining is then determined by summing the damage of all "n" load cycles as:

$$D_e = \sum_{i=1}^{n} D^i = \sum_{i=1}^{n} \left(\frac{\Delta_i}{\Delta u_i}\right)^{\alpha_i} \tag{3.2}$$

This damage model was used to estimate the potential damage of metal structures subjected to strong seismic motions, i.e. by Kasiraj and Yao(17) for deterministic loading conditions(1940 El Centro N/S earthquake), and by Tang and Yao(40) for random loading conditions. Recently, Stephens and Yao(39) modified this damage model for reinforced concrete members. This model will be discussed in Section 3.4.7. However, it can already be pointed out that it does not consider the effect of the loading sequence, which has been shown to have a potentially important

influence on the damage of reinforced concrete members. Also, the experimental determination of Δu_i and α_i, is very difficult for nonhomogeneous RC members.

3.1.2 Oliveira(1975)

For monotonic loading, Oliveira(24) proposed the following damage ratio:

$$D_e = \left(\frac{\Delta}{\Delta u}\right)^{\alpha} \tag{3.3}$$

where

Δ : largest plastic deformation(demand) resulting from the load

Δu : ultimate plastic deformation(capacity) of the member

α : nonnegative parameter depending on the material properties

Also, this damage expression can not be directly used for RC members because it ignores many important factors, such as energy dissipation and loading history.

3.1.3 Krawinkler and Zohrei(1983)

Recently, Krawinkler and Zohrei(18) proposed an accumulated damage model for structural steel components based on experimental data so as to assess the reliability of structures subjected to severe ground motions.

$$D_e = C \sum_{i=1}^{n} (\Delta\delta_{pi})^{\alpha_i} \tag{3.4}$$

where

D_e : damage index of the member

C, α_i : damage parameters

n : number of load cycles

$\Delta\delta_{pi}$: plastic deformation during the i $-$ th cycle

For constant amplitude cycling, the strength drop per cycle is assumed to be $\Delta_s = A(\Delta\delta_p)^a$ where $\Delta\delta_p$ denotes the plastic deformation range, and A and a are structural damage parameters. The total number of cycles to failure with constant load amplitude is then $N_f = \frac{x}{A\,(\Delta\delta_p)^a}$ where x is the strength drop which corresponds to the definition of failure. Using Miner's rule, i.e. the assumption of linearly accumulated damage, the damage index can be obtained as:

$$D_e = \sum_{i=1}^{n} \frac{1}{N_{fi}} = C \sum_{i=1}^{n} (\Delta\delta_{pi})^{\alpha_i} \tag{3.5}$$

The concept of this model seems to be very attractive for the derivation of a rational damage model for RC members, provided that it includes a damage acceleration factor which reflects the effect of the loading sequence. Similarly this model as proposed is valid for a material whose inelastic behaviour is almost similar in tension and compression. Thus, it has to be modified appropriately before it can be used for reinforced concrete members.

3.2 Empirical Damage Definitions

Empirical damage definitions are commonly based on more or less subjective observations of building damage. Because they all but disregard the mechanics of materials that undergo large inelastic cyclic loads, they do not lend themselves to rationally predicting the strength reserve and response characteristics of a structure with a specified degree of damage. They tend to reflect statistical averages and as such may be of use for purposes other than the objective of our study.

3.2.1 Seed et al(1970)

Seed et al(37) proposed an empirical procedure for the damage assessment of existing buildings based on the observation of building damage caused by the 1967 Caracas earthquake. The overall seismic damage is represented by the number of

buildings that suffered structural damage divided by the total number of buildings. The damage caused by this earthquake was shown to clearly correlate with the soil conditions and in effect was attributed to the rocking of the foundations.

3.2.2 Whitman et al(1972-74)

Whitman et al(42,43,44) proposed a method for grading existing buildings based on the damage data from the 1971 San Fernando earthquake. The severity of ground motion is represented by the MMI scale, and the overall seismic damage is expressed as the ratio of repair cost to the replacement cost of a building.

Similar empirical approaches have been used by other investigators, such as Wiggins and Moran(45), Earthquake Engineering Systems(12), Blume et al(7), Sauter et al(34), Hafen and Kintzer(14), Wong et al(47). All of these may be of value for nonengineering purposes such as insurance risk evaluation. For structural analysis purposes they are of little interest.

3.2.3 Blume et al(1975)

Blume et al(41) proposed the spectral matrix method(SMM) and the seismic element method(SEM) for potential damage assessment of a building or a group of buildings. Ground motion characteristics are represented by the mean pseudo-velocity response spectrum, and the structural capacity is expressed by the base shear at yielding. The basic procedure for the SMM method is as follows.

1) A mean damage factor curve is generated for each building type.
2) The curve relates damage to a normalized ratio of median demand over mean capacity for specified values of the other capacity parameters.
3) The overall damage is expressed as the ratio of repair cost to the replacement cost.

The SMM method also makes use of probabilistic formulations for individual build-

ing demand and capacity. Similar attempts have been also made by Culver et al(9), Czarnecki et al(8) and others.

3.3 Energy Indices for RC Members

As was discussed in Chapter 2, the hysteretic energy dissipated by RC members plays a vital role in the damage sustained during cyclic loading and thus their reserve strength. In recognition of this importance, various normalized energy indices have been proposed in the past. Before reviewing theoretical damage models for RC members, we will therefore discuss these indices in some detail and investigate their applicability for damage models for RC members in the subsequent section.

3.3.1 Gosain et al(1977)

Gosain et al(13) proposed a work index, I_w, which is a normalized dissipated energy index and as such a measure of the energy absorption capacity of reinforced concrete components subjected to strong cyclic loadings. Since the load range varies from $p_i = 0.75p_y$ to $p_i = 1.25p_y$ and thus $p_i = p_y$ on the average, it can be also simplified as shown below.

$$I_w = \sum_{i=1}^{n} \frac{p_i \Delta_i}{p_y \Delta_y} = \sum_{i=1}^{n} \frac{\Delta_i}{\Delta_y} \tag{3.6}$$

where

n : number of load cycles with $p_i \geq 0.75p_y$

p_i, Δ_i : load and corresponding displacement during $i-th$ cycle

p_y, Δ_y : load and corresponding displacement at yield of flexural bars

For pure bending, Eq (3.6) appears to be an appropriate measure of dissipated energy. However, in the presence of high shear forces, the load-deformation curves tend to assume a pinched shape, with a considerable reduction of the dissipated

energy, Fig. 2.1. On the other hand, in the presence of small axial compression forces, load-deformation curves tend to be more stable over a larger number of load cycles, thus increasing the energy absorption capacity of a member. In order to account for these factors, Gosain et al(13) have modified their work index as:

$$I'_w = I_w \left(1 - \frac{d_c}{a}\right) \left(1 + \frac{0.0005N}{A_{core}}\right) \tag{3.7}$$

where

$\frac{a}{d_c}$: shear span ratio

N : axial force

A_{core} : core area of the section

It can be observed that even this modified work index does not consider effects of the loading history, the strength of concrete, the confinement ratio, etc, which do contribute to the amount of dissipated energy. Also, the questionable assumptions concerning the linear effects of shear span ratio and axial force may be responsible for the high degree of scatter displayed by experimental data.

3.3.2 Hwang and Scribner(1984)

After reviewing Gosain's work index, Hwang(15,16) suggested the following normalized energy index.

$$I_E = \sum_{i=1}^{n} E_i \cdot \frac{k_i}{k_e} \cdot \left(\frac{\Delta_i}{\Delta_y}\right)^2 \tag{3.8}$$

where

E_i : energy dissipated during the i − th cycle

k_e, Δ_y : elastic stiffness and yield deflection, respectively, Fig.3.2

k_i, Δ_i : flexural stiffness and max. deflection in i − th cycle, respectively

n : number of cycles with $P_i \geq 0.75P_y$

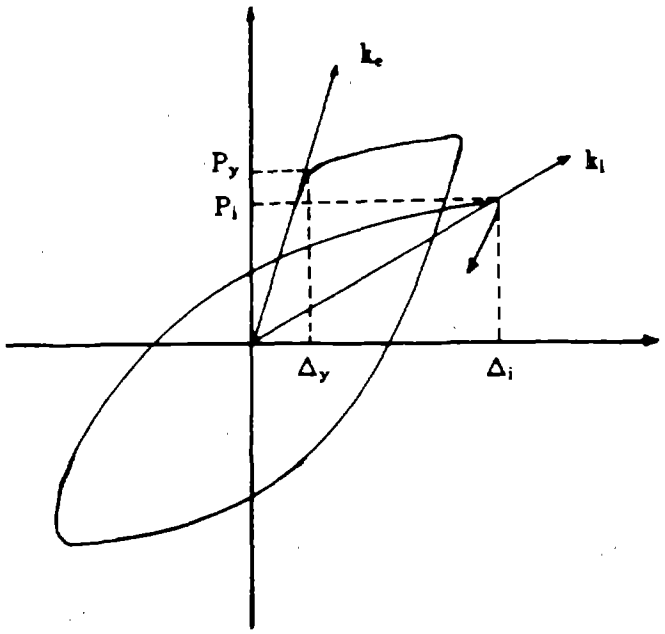

Fig. 3.2 - Definition of k_e, k_i, Δ_y and Δ_i (Ref. 15)

On the basis of their own and other researcher's experimental data, Hwang and Scribner assumed a linear relationship between $\frac{v_m}{\sqrt{f'_c}}$ and the logarithm of their energy index, using linear regression analysis, Fig. 3.3, where v_m is the maximum shear stress.

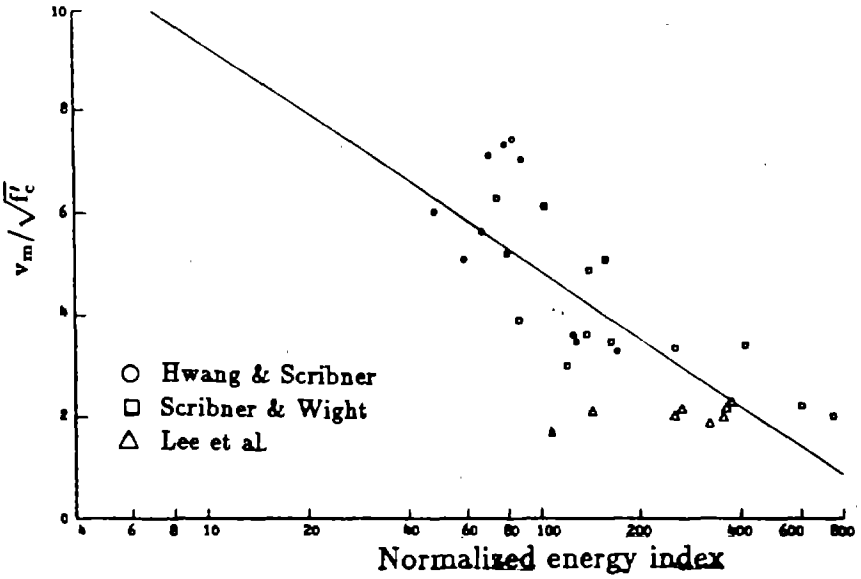

Fig. 3.3 - $v_m/\sqrt{f'_c}$ versus normalized energy index(Ref. 15)

The relatively high scatter of data points suggests that the assumed functional relationship disregards other important influence factors. Even though experimental data obtained with reinforced concrete members, especially under strong cyclic loads, do exhibit a certain unavoidable amount of scatter, it is felt that shear stress and work index are poor choices to establish a functional relationship such as displayed in Fig. 3.3. It is noteworthy that Hwang, after having introduced the work index in Ref.(15), has abandoned it in favor of Gosain's work index in Ref.(16).

3.3.3 Darwin et al(1986)

Darwin(10,23) also investigated the relationship between various controlling parameters and the dissipated energy index, defining the energy index as the ratio of total dissipated energy divided by the elastic strain energy both in tension and compression.

$$E_i = \frac{E}{0.5\ p_y\ \Delta_y\ \left(1 + \left(\frac{A'_s}{A_s}\right)^2\right)} \tag{3.9}$$

where

E_i : normalized dissipated energy index

E : total dissipated energy

A'_s, A_s : area of compression and tension steel, respectively

Using linear regression analysis, Darwin found a linear relationship between D_i and $\frac{(v_s\ f'_c)^{0.5}}{v_m^{1.5}}$.

$$D_i = 222\ \frac{(v_s\ f'_c)^{0.5}}{v_m^{1.5}} - 17 \tag{3.10}$$

where

$v_s = \frac{A_v\ f_{vy}}{bs}$; shear reinforcement capacity

v_m : maximum applied shear stress

A_v : stirrup area

f_{vy} : stirrup yield strength

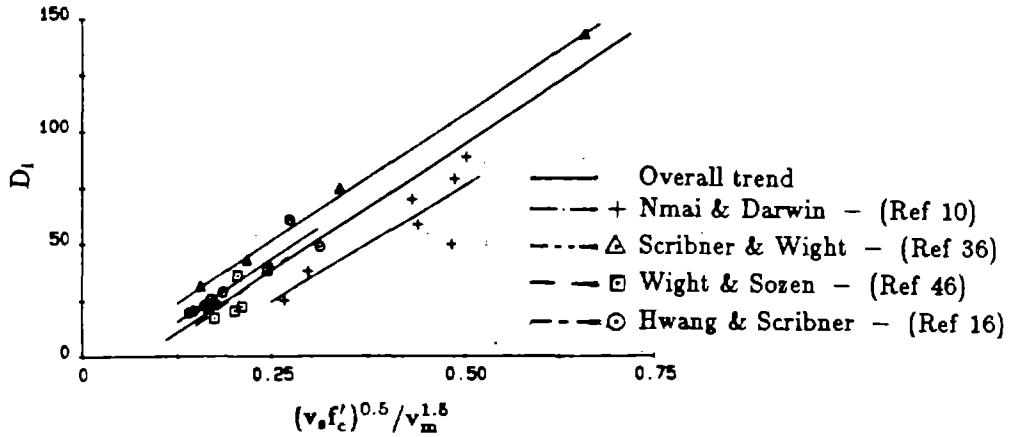

Fig. 3.4 - Energy dissipation index, D_i, versus $(v_s f'_c)^{0.5}/v_m^{1.5}$ (Ref. 23)

Even though the statistical scatter of data points for this functional relationship is considerably less than for the other proposed indices, Fig. 3.4, it is obvious that the shear stress and shear capacity are important but not the only important parameters that affect the energy absorption capacity of RC members.

3.4 Damage Models for RC Members Based on Theoretical Principles

Numerous damage models for RC members have been proposed in the past, which recognize the importance of the dissipated energy. In order to derive global damage measures for entire structures(D_g), some investigators combined the local damage indices for individual components(D_e) using some weighting factors. Before presenting our own model in Chapter 4, we will therefore discuss these theoretical models in some detail, point out those features that are compatible with physical observations and theoretical considerations; and we shall also comment on those aspects that should but have not been included in these models.

3.4.1 Lybas and Sozen(1977)

Lybas and Sozen(20) introduced a damage ratio as follows, Fig. 3.5.

$$D_R = \frac{k_o}{k_r} \tag{3.11}$$

where

k_o : initial tangent stiffness

k_r : reduced secant stiffness corresponding to max displacement

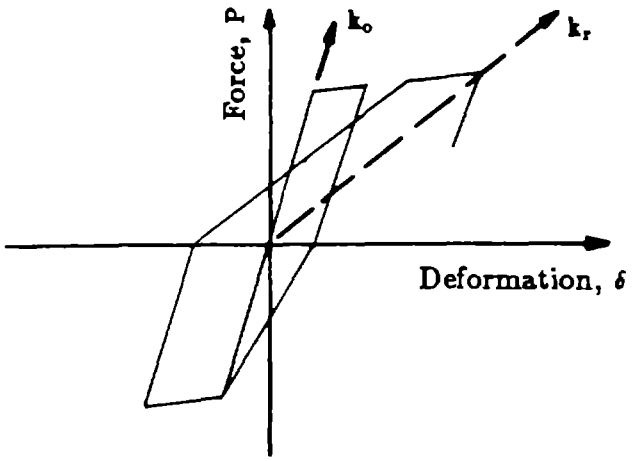

Fig. 3.5 - Definition of k_o and k_r(Ref. 20)

It is obvious that a simple ratio as this one is not capable of simulating the pinching effect due to high shear stress and completely disregards any effect that the load history may have. For these reasons it appears to be an inadequate measure of damage for the purpose of predicting residual strength and energy absorption capacity.

3.4.2 Bertero and Bresler(1977)

Bertero and Bresler(5) introduced relationships between local damage(D_e), global damage(D_g) and cumulative damage(D_t). By local damage is meant the damage of a constituent component of a structure expressed as the ratio of the

maximum response to the cumulative deformation capacity, i.e. $D^i = \frac{d_i}{c_i}$, where d_i is the response(or demand) due to the load, and c_i is the resistance(or capacity) of the i-th component. By global damage is meant the building damage defined as a combination of local damage indices with certain weighting factors. Cumulative damage is the result of a series of strong cyclic load exposures and defined as:

$$D_t = \frac{1}{\Sigma w_i} \cdot \left(\sum_{i=1}^{m} \frac{w_i \gamma_i d_i}{\chi_i c_i} \right) \tag{3.12}$$

where

D_t : cumulative damage index

w_i : importance weighting factor for i − th structural component

χ_i : service history influence coefficient for demand

γ_i : service history influence coefficient for capacity

Also, this damage model does not consider the effects of shear span ratio, confinement ratio, etc, and the influence of load history is accounted for inadequately. The determination of w_i, χ_i and γ_i requires experienced engineering judgement, which is the source of high uncertainty in the result. Particularly, the local damage index is a kind of ductility ratio, which is not sufficient as a reliable measure of the low-cycle fatigue strength of RC structures.

3.4.3 Blejwas and Bresler(1979)

In addition to the various damage indices of the previous section, Blejwas and Bresler(6) presented an alternative definition of local, global and cumulative damage indices by using a quasi-static structural analysis method, which adopts a single-degree-of freedom analogy for predicting earthquake damage. Local damage for an element is expressed as:

$$D^i = \frac{d_i - c_i^o}{c_i^u - c_i^o} \qquad 1 \geq D^i \geq 0 \tag{3.13}$$

where

D^i : local damage index for i – th component

d_i : demand parameter, formed as a combination of response parameters

c_i^o : capacity at which damage is initiated(calculated or a best guess)

c_i^u : capacity at which damage is irrepairable(a best guess)

While this damage index seems to be a more realistic definition of damage than that of the previous section, it is necessary to use engineering judgement to perform further calibration studies for various parameters and capacity bounds to make this method more practical and useful. Also, this damage model does neither consider the effects of shear span ratio, confinement ratio, etc, nor the influence of individual load history. Thus, this model is not a reliable measure of damage of RC structures.

3.4.4 Banon et al(1980)

Banon et al(2,3,4) summarized various damage ratios for structural components and proposed a global damage index using probabilistic concepts. The most widely used damage indicators for structural components are expressed in the form of ductility ratios, i.e.

1) $\mu_\theta = \frac{\theta_{max}}{\theta_y}$: rotational ductility, where θ_{max}, θ_y are the maximum and yield rotation, respectively;
2) $\mu_\phi = \frac{\phi_{max}}{\phi_y}$: curvature ductility, where ϕ_{max}, ϕ_y are the maximum and yield curvature, respectively;
3) $FDR = \frac{k_f}{k_r}$: flexural damage ratio, where k_f, k_r are the initial flexural stiffness(instead of k_o) of a cracked member and a reduced secant stiffness at maximum displacement, respectively, Fig. 3.1. This seems to be a better predictor of damage than the other two ratios, because the reduced secant stiffness, k_r, reflects both strength and stiffness degradation.

Neither of the three damage indicators, however, reflects the cumulative damage incurred during the dissipation of energy. As a result, Banon proposed the following cumulative damage parameters:

1) $NCR = \frac{\Sigma|\theta_o|}{\theta_y}$: Normalized cumulative rotation, defined as the ratio of the absolute sum of all plastic rotations(except for those associated with unloading) to the yield rotation.

2) $E_n(t) = \frac{\int_0^t M(\tau)\theta(d\tau)}{M_y \frac{\theta_y}{2}}$: Normalized dissipated energy as a function of time, defined as the energy that is dissipated up to time "t", divided by maximum energy that can be stored elastically.

The values of FDR and $E_n(t)$, designated as D_1 and D_2, respectively, can now be considered to be state variables, so that specific damage states, including failure, can be represented by surfaces. For example, Fig. 3.6 illustrates the load paths in the $FDR - E_n(t)$ plane, including the failure states for five different test specimens. By transforming the damage state variables as $D_1^* = D_1 - 1$ and $D_2^* = b \cdot D_2^r$ (the choice of $r = 0.38$ and $b = 1.1$ linearizes the paths in the transformed plane), lines of equal probability of failure(contours) can be constructed, Fig. 3.7.

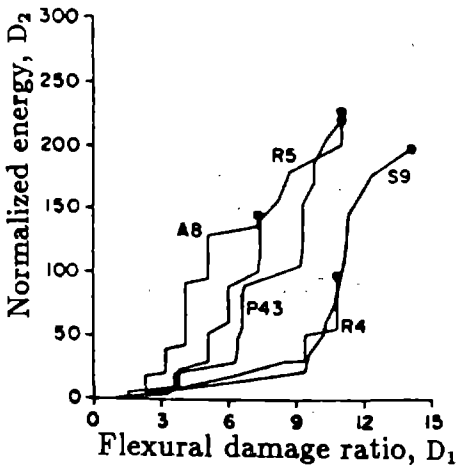

Fig. 3.6 - Experimental damage trajectories up to failure(Ref. 4)

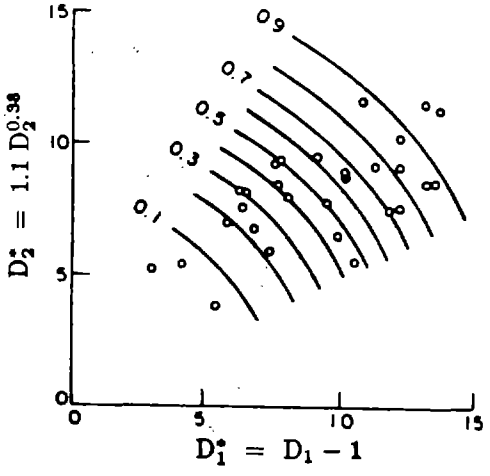

Fig. 3.7 - Contours of equal probability of failure and experimental failure points in (D_1^*, D_2^*) plane(Ref. 4)

Taking into consideration the different responses of RC members in tension and compression, appropriate weighting factors for the normalized dissipated energy must be introduced. The choice of r and b appears to be somewhat arbitrary, as it is based on a small number of test data. This is probably the reason for the high degree of scatter of the damage prediction. Still, the concept of combining the energy dissipation and flexural damage ratio is an important step in recognition of the actual behaviour of RC members.

3.4.5 Roufaiel and Meyer(1985)

Roufaiel and Meyer(31,32,33) used the modified flexural damage ratio, which involves secant stiffnesses at the onset of failure, (M_m, ϕ_m), at the time of yield (M_y, ϕ_y), and some arbitrary load level (M_x, ϕ_x), as follows, Fig. 3.8,

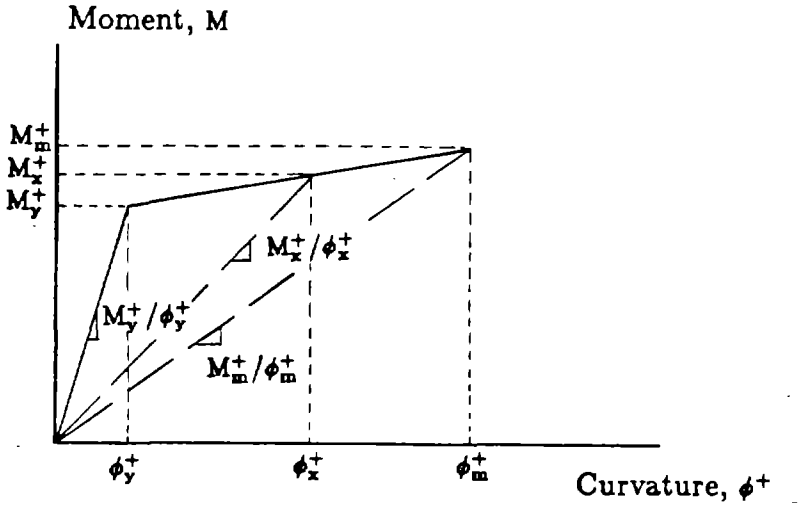

Fig. 3.8 - Definition of modified flexural damage ratio(Ref. 33)

$$MFDR = max\,[MFDR^+, MFDR^-] \tag{3.14}$$

$$MFDR^+ = \frac{\frac{\phi_x^+}{M_x^+} - \frac{\phi_y^+}{M_y^+}}{\frac{\phi_m^+}{M_m^+} - \frac{\phi_y^+}{M_y^+}}, \qquad MFDR^- = \frac{\frac{\phi_x^-}{M_x^-} - \frac{\phi_y^-}{M_y^-}}{\frac{\phi_m^-}{M_m^-} - \frac{\phi_y^-}{M_y^-}} \tag{3.15}$$

In addition, a global damage parameter, GDP, was introduced as follows.

$$GDP = \frac{d_R - d_Y}{d_F - d_Y} \tag{3.16}$$

where

d_R : maximum roof displacement

d_Y : roof displacement at the yield of the first member

d_F : roof displacement at the failure of structure

The yield roof displacement, d_Y, is based on the first mode of the deformation of the frame, and as an estimation of failure displacement, extracted from various tests, $d_F = 0.06\ H$ is suggested, where H is the building height. This kind of damage ratio, that is the ratio between certain stiffness factors, does not consider the effect of cumulative damage, and therefore cannot serve as a reliable damage predictor for RC members. However, it does consider the different responses of RC members to positive and negative bending.

3.4.6 Park et al(1985)

The damage model proposed by Park et al(25,26,27) assumes the total damage to be a linear combination of the damage caused by excessive deformation and the damage caused by dissipation of energy.

$$D_e = \frac{\delta_{max}}{\delta_u} + \frac{\beta}{Q_y \delta_u} \int dE \tag{3.17}$$

where

δ_{max} : maximum deformation experienced so far

δ_u : ultimate deformation under monotonic loading

Q_y : calculated yield strength

dE : dissipated energy increment

and

$$\beta = \left(-0.447 + 0.73\frac{l}{d} + 0.24n_o + 0.314P_t\right) 0.7^{\rho_w} \tag{3.18}$$

where

$\frac{l}{d}$: shear span ratio

n_o : normalized axial force

ρ_w : confinement ratio

P_t : longitudinal steel ratio

The various numerical factors in Eq (3.18) were obtained by regression analysis of numerous experimental data. As a global damage index, Park suggested a combination of individual member damage indices, using the dissipated energies as weighting factors:

$$D_g = \frac{\sum_i D_e^i \cdot E_i}{\sum_i E_i} \tag{3.19}$$

where

D_g : global damage index

E_i : total energy dissipated by the i − th member

D_e^i : local damage index of i − th member

In a weak-column and strong-beam structure, an individual story damage index can serve as global damage index according to Eq (3.19). In a structure designed with strong columns and weak beams, the summation in Eq (3.19) has to extend over the entire structure.

In evaluating the damage index of Eq (3.17), it is apparent that a significant role is assigned to the function β, which depends on four completely unrelated variables.

It is debatable whether a straight linear accumulation of influence factors such as given in Eq (3.18) pays due respect to the physical characteristics of reinforced concrete suffering damage due to cyclic loads. More significant is the stipulation of linear superposition of the two terms in Eq (3.17). Because maximum displacement and dissipated energy are closely related to each other, the form of Eq (3.17) seems to be inappropriate. It suggests that these two variables were linearly independent, which, of course, they are not.

3.4.7 Stephens et al(1987)

Stephens et al(39) proposed a damage model, which is a modification of the damage index proposed by Yao and Munse(48) for metals. This damage index is a simple accumulation of plastic deformation experienced during load cycling.

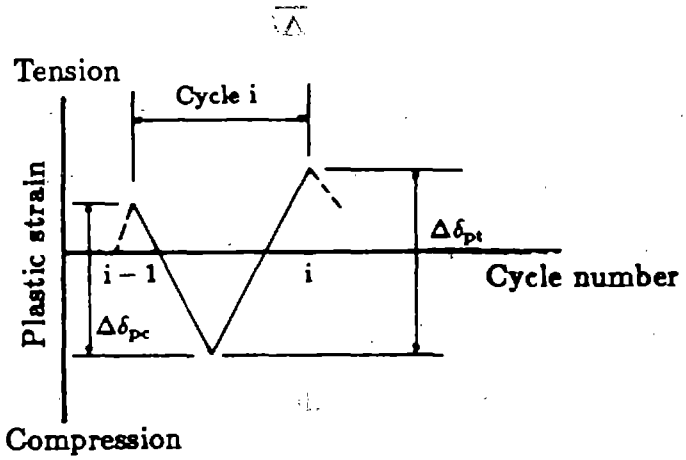

Fig. 3.9 - Typical response cycle for reinforced concrete(Ref. 39)

$$D_e = \sum_{i=1}^{n} D^i \tag{3.20}$$

where

$$D^i = \left(\frac{\Delta\delta_{pt}}{\Delta\delta_{pf}}\right)^{\alpha} \tag{3.21}$$

is the damage index for load cycle i, and:

D_e : damage index for all n cycles, respectively

$\alpha = 1 - b * rl$: fatigue exponent coefficient

b : deformation ratio coefficient

$rl = \frac{\Delta\delta_{pc}}{\Delta\delta_{pt}}$

$\Delta\delta_{pt}$: positive change in plastic deformation in cycle i, Fig.3.9

$\Delta\delta_{pf}$: max. change in plastic deformation to cause failure, Fig.3.9

On the basis of the following simplifying assumptions, $\alpha = 1.77$, $b = 0.77$, and $\Delta\delta_{pf} = \Delta\delta_{mf}$, D^i appears as:

$$D^i = \left(\frac{\Delta\delta_{pt}}{\Delta\delta_{mf}}\right)^{1.77} \tag{3.22}$$

As already mentioned in section 3.1.1., the determination of $\Delta\delta_{pf}$ and α_i for reinforced concrete members is very difficult and subject to large statistical scatter, which reduces the usefulness of this damage model.

3.4.8 Mizuhata and Nishigaki(1987)

Similarly as in the Park's model, the model proposed by Mizuhata and Nishigaki(51) assumes that the local damage of an RC member is the sum of the damage caused by maximum displacement experienced and the damage accumulated by repeated cyclic loading.

$$D_e = \frac{|\delta_{max}|}{\delta_F} + \begin{cases} \sum_{i=1}^{k} \left(\frac{n_i}{N_{fi}}\right)^{0.715} \cdot 0.609 \cdot \left(1 - \frac{\delta_i}{\delta_F}\right) & \text{for } 0.078 \geq \frac{n_i}{N_{fi}} > 0 \\ \sum_{i=1}^{k} \left(\frac{n_i}{N_{fi}}\right)^{0.910} \cdot \left(1 - \frac{\delta_i}{\delta_F}\right) & \text{for } 1.0 \geq \frac{n_i}{N_{fi}} > 0.078 \end{cases} \tag{3.23}$$

where

δ_i : specified displacement level

k : number of different displacement levels

n_i : number of cycles at with displacement level, δ_i

N_{fi} : number of cycles to failure with displacement level, δ_i

δ_{max} : maximum displacement experienced

δ_F : displacement at failure under monotonic loading

This equation has been derived on the basis of low-cycle fatigue tests performed under constant displacement amplitudes. For the derivation, the following steps were taken:

1) The fatigue damage accumulated during cyclic loading with constant displacement amplitude δ_i can be defined as the ratio of dissipated energies,

$$D_E(n_i) = \sum_{k=1}^{n_i} \frac{E_k}{E_T} \tag{3.24}$$

where

E_k : energy dissipated in k − th cycle with displacement level, δ_i

n_i : number of actually experienced load cycles of level, δ_i

E_T : total energy dissipation capacity

2) On the assumption of linearly accumulated damage, Eq (3.24) could be written with $E_T = N_{fi}E_i$ and $\sum_{k=1}^{n_i} E_k = n_i E_i$ as

$$D(n_i) = \frac{n_i E_i}{E_T} = \frac{n_i}{N_{fi}}$$

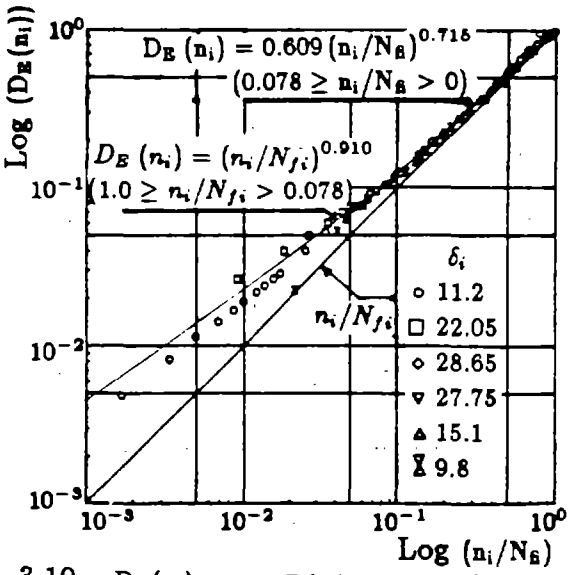

Fig. 3.10 - $D_E(n_i)$ versus $D(n_i) = n_i/N_f$ (Ref. 52)

According to test results, however, $D(n_i) \neq D_E(n_i)$, Fig. 3.10. These two damage measures rather appear to be related as follows,

$$D_E(n_i) = \begin{cases} 0.609 \cdot (\frac{n_i}{N_{fi}})^{0.715} & \text{for} \quad 0.078 \geq \frac{n_i}{N_{fi}} > 0 \\ (\frac{n_i}{N_{fi}})^{0.910} & \text{for} \quad 1.0 \geq \frac{n_i}{N_{fi}} > 0.078 \end{cases} \tag{3.25}$$

3) The seismic damage index of Eq (3.24) is then formed as the sum of the damage caused by maximum displacement experienced, $\frac{|\delta_{max}|}{\delta_y}$, and the damage accumulated by repeated loadings to account for the phenomenon of low-cycle fatigue. Different displacement levels δ_i are accounted for in the form of a modified Miner's rule, by applying non-unity exponents to the $\frac{n_i}{N_{fi}}$ ratios, and by multiplying them with the factor $(1 - \frac{\delta_i}{\delta_y})$, as indicated in Eq (3.23).

The basic concept of the Mizuhata-Nishigaki model is the same as that of the Park-Ang model of Section 3.4.6 in that the damage is assumed as the sum of the damage caused by maximum displacement experienced and the damage accumulated by repeated cyclic loading. But there are two important differences:

1) For the evaluation of damage caused by low-cycle fatigue loading,

Mizuhata-Nishigaki's model employs a modified Miner's rule by introducing the

factor $(1 - \frac{\delta_i}{\delta_F})$, while Park-Ang's model expresses the incremental dissipated energy as a simple function of the non-negative parameter β.

2) Mizuhata-Nishigaki's model is based on the failure displacement, δ_F, determined from actual monotonic test, while Park-Ang's model uses the less accurately definable numerical expression $\delta_f = \mu_u \cdot \delta_y$, where $\delta_y = \delta_f + \delta_b + \delta_s + \delta_e$, and

μ_u : ductility factor

δ_y : yield displacement

δ_f : displacement due to flexure

δ_b : displacement due to bond deterioration

δ_e, δ_s : elastic and inelastic shear displacement, respectively

δ_F : failure displacement

As the preceding discussion shows, many different damage models have been proposed in the past. However, judging on the basis of the general discussion of damage presented in Chapter 2, none of these models appears to recognize all of the important physical aspects associated with damage and failure of concrete members under cyclic loads. In the following chapter, we shall present a new damage model which we believe does take all of these considerations into account.

4. A New Damage Model

Many attempts have been made to develop damage models which are somewhat related to the amount of macroscopic cracking. Some of these are tied to the energy dissipated during cyclic loading, others are based on the stiffness degradation or accumulation of plastic deformation, and again others employ a linear combination of dissipated energy and some normalized displacement. Herein, a new damage model shall be proposed, which reflects the role that damage plays in defining the residual strength reserves of RC members. As a prerequisite, details of the hysteretic behaviour model shall be described, followed by definitions of strength deterioration, the influence of shear, and failure.

4.1 Mathematical Model for Hysteretic Behaviour

Under load reversals, the stiffness of a RC member experiences a progressive reduction due to cracking of the concrete and bond deterioration of the steel-concrete interface. The models that have been proposed to describe this behaviour can be categorized into bilinear, bilinear degrading, and trilinear models.

Herein, the trilinear model proposed by Roufaiel and Meyer(31) will be modified, Fig. 4.1. It is characterized by five different kinds of branches:

1) Elastic loading and unloading: If the maximum moment does not exceed the yield moment M_y, the moment-curvature relationship is

$$\Delta M = (EI)_1 \Delta\phi \tag{4.1}$$

where

$$(EI)_1 = (EI)_e \tag{4.2}$$

is the initial elastic member stiffness.

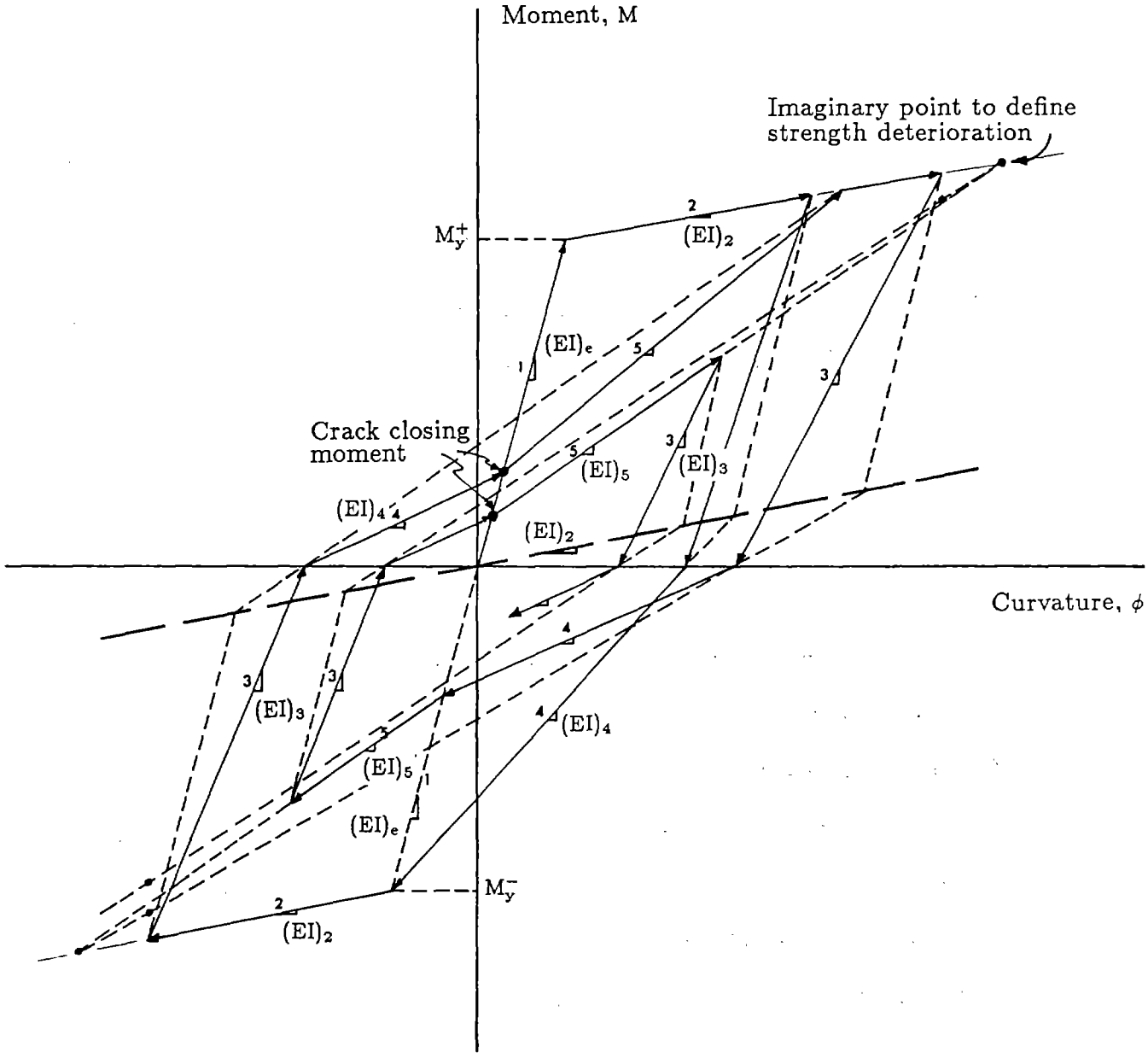

Fig. 4.1 - Typical hysteretic moment-curvature relationship

2) Inelastic loading: If the moment exceeds the yield moment and is still increasing(see Fig. 4.2), the moment-curvature relationship is

$$\Delta M = (EI)_2 \Delta\phi \tag{4.3}$$

where

$$(EI)_2 = p(EI)_e \tag{4.4}$$

$$p(EI)_e = \frac{M_u - M_y}{\phi_u - \phi_y} \tag{4.5}$$

3) Inelastic unloading: If the moment decreases after the yield moment has been exceeded(Fig. 4.2), the moment-curvature relationship is

$$\Delta M = (EI)_3 \Delta\phi \tag{4.6}$$

where

$$(EI)_3 = \frac{M_x}{\phi_x - \phi_r^+} \tag{4.7}$$

The "+" superscript denotes loading in the positive sense. Likewise, a "-" superscript stands for negative loading.

4) Inelastic reloading during closing of cracks: In a reversed load cycle, previously opened cracks tend to close, leading to an increase in stiffness and a characteristic "pinched" shape of the moment-curvature curve. This effect is a function of the shear span. If the absolute value of the moment increases but is still less than a certain "crack-closing moment" M_p^+(see Fig. 4.3), the moment-curvature relationship is

$$\Delta M = (EI)_4 \Delta\phi \tag{4.8}$$

where

$$(EI)_4 = \frac{M_p^+}{\phi_p^+ - \phi_r^-} \tag{4.9}$$

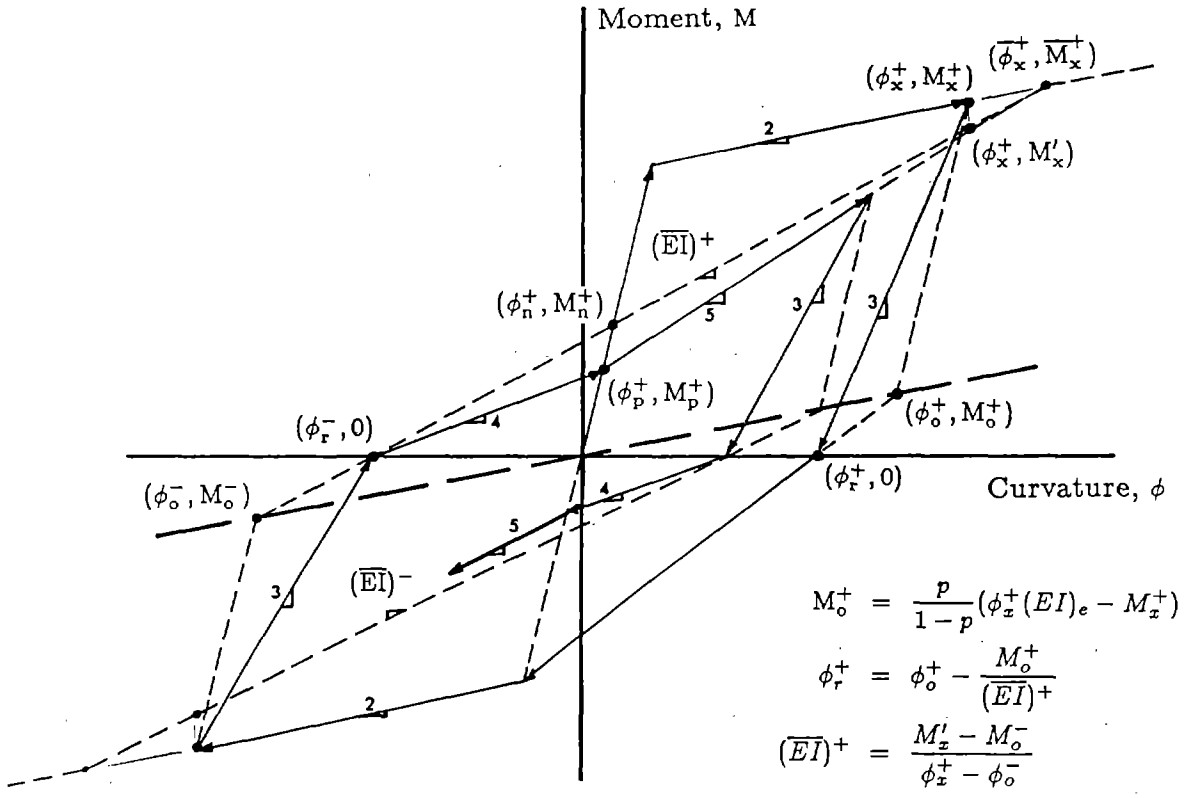

Fig. 4.2 - Computational procedure for inelastic deterioration

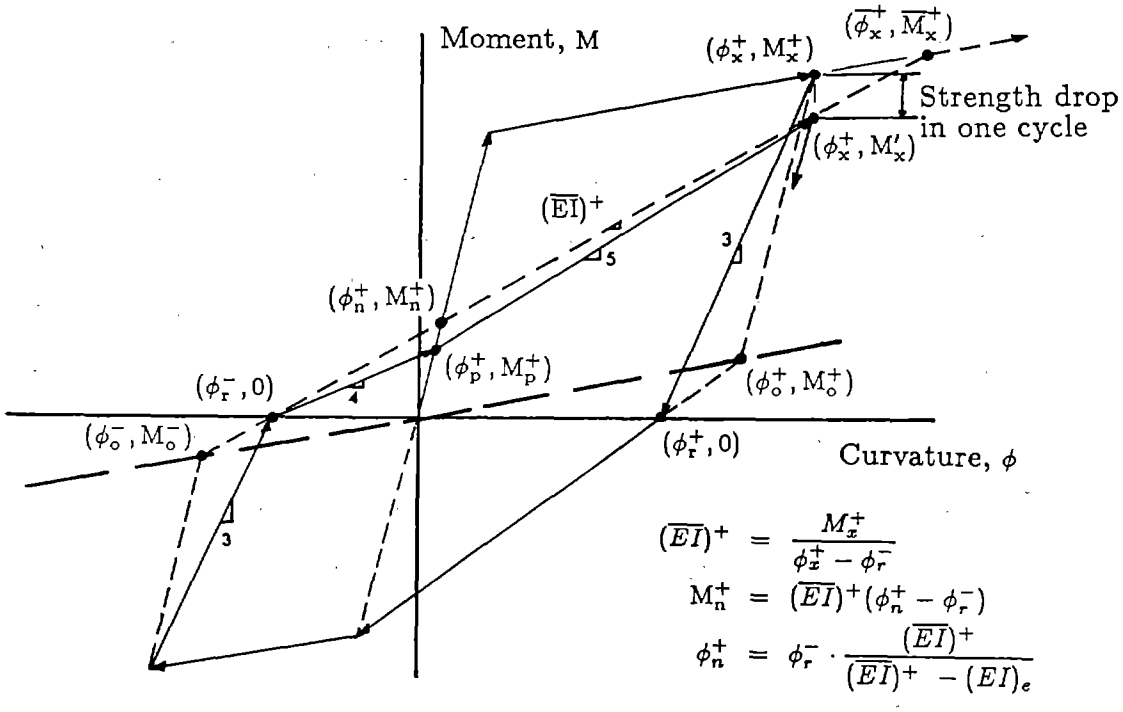

Fig. 4.3 - Typical crack closing moment and strength deterioration

5) Inelastic reloading after closing of cracks: Once the absolute value of the moment exceeds the "crack-closing moment" M_p^+, and is still increasing, then the moment-curvature relationship is

$$\Delta M = (EI)_5 \Delta\phi \tag{4.10}$$

where

$$(EI)_5 = \frac{\overline{M}_x - M_p^+}{\overline{\phi}_x - \phi_p^+} \tag{4.11}$$

4.2 Strength Deterioration

In addition to stiffness degradation, RC members experience strength deterioration under cyclic loading beyond the yield level. The rate of strength deterioration and the failure curvature depend on many factors, such as the confinement ratio, axial force, concrete strength etc. If the failure curvature for monotonic loading ϕ_f, is known, it is possible to derive a strength deterioration curve, as will be shown below. The numerical procedure for determining ϕ_f is detailed in Appendix A.

Atalay and Penzien(1) had noticed some correlation between commencement of strength deterioration and the spalling of the concrete cover. But Hwang's experiments showed that strength deterioration can start at considerably lower load levels. Even for loads slightly above the yield level, damage and strength deterioration can be observed, provided a sufficiently large number of load cycles is applied. Roufaiel(31) found a strong correlation between the onset of strength deterioration and a "critical" displacement level, at which the concrete in the extreme compression fibre is strained to some limit value. But his investigation relied on test data with relatively small numbers of cycles for each load level, such as the test series by Ma et al(21). More significantly, it is unreasonable to stipulate such a precisely defined point of failure initiation, i.e. to say if this point is exceeded by a small

amount, strength deterioration is initiated, but if it is missed by a small amount, no such strength deterioration takes place. It is, therefore, suggested that strength deterioration is initiated as soon as the yield load level is exceeded, and the strength deterioration accelerates as the critical load level is reached. For this purpose, a strength drop index, S_d, is proposed which defines the strength drop to be expected for a given curvature, ϕ, in a single load cycle(see Fig. 4.4).

$$\begin{aligned} S_d &= \frac{\Delta M}{\Delta M_f} \\ &= A \cdot \left[\left(\frac{\phi}{\phi_u}\right)^{2\omega} + B\left(\frac{\phi}{\phi_u}\right)^{\omega} + C \right] \end{aligned} \tag{4.12}$$

where

S_d : strength drop index for curvature ϕ in a single load cycle

ΔM : moment capacity(strength) reduction for curvature ϕ in a single load cycle

ΔM_f : moment capacity(strength) reduction in a single load cycle at failure curvature

ϕ_u : curvature corresponding to ultimate moment capacity M_u

A, B, C, ω : free constants

With ΔM denoting the strength drop in one load cycle for some curvature ϕ, the residual strength after this one load cycle is given by

$$\begin{aligned} m_1(\phi) &= M(\phi) - \Delta M \\ &= M_y + (\phi - \phi_y)\ p(EI)_e - S_d\ \Delta M_f \end{aligned} \tag{4.13}$$

and is illustrated in Fig. 4.4. Similarly, one would obtain for i load cycles, the residual strength

$$m_i(\phi) = M(\phi) - i \cdot \Delta M \tag{4.14}$$

Some of the free constants in Eq (4.12) can be determined from known boundary conditions:

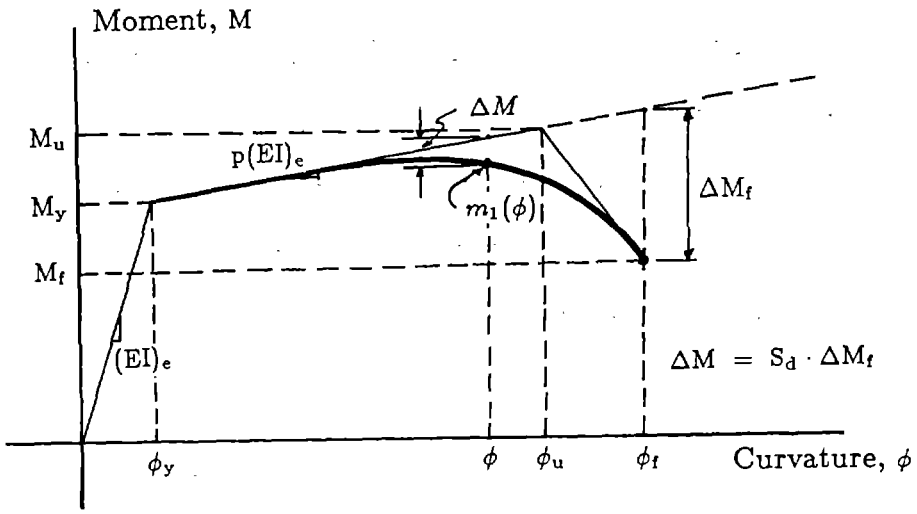

Fig. 4.4 - Strength deterioration curve

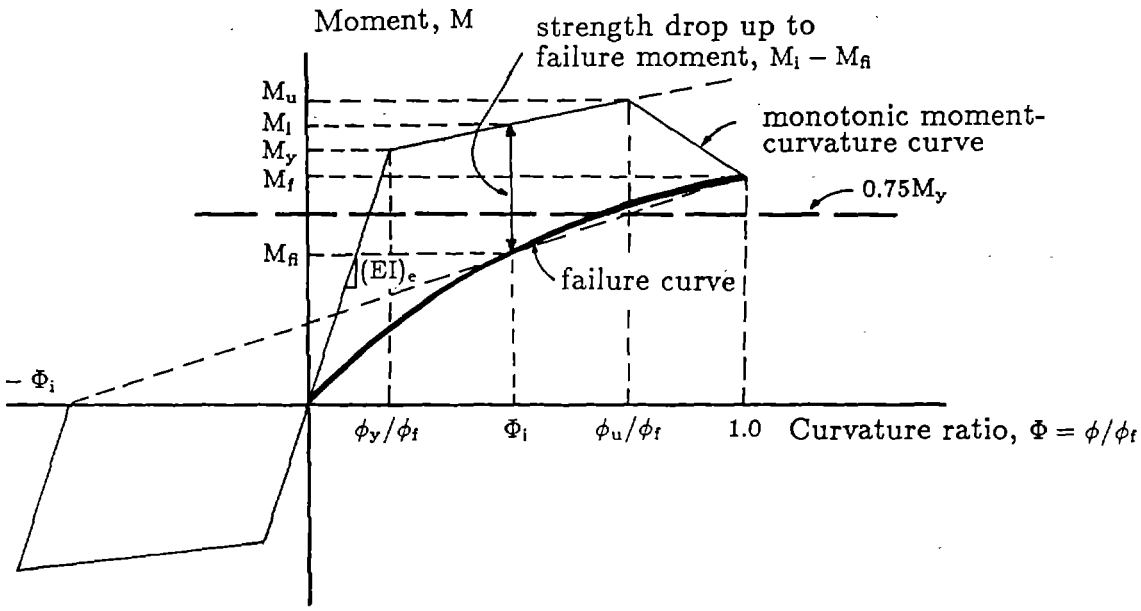

Fig. 4.5 - Definition of failure

1) $\Delta M = 0$ at $\phi = \phi_y$, i.e.

$$S_d|_{\phi=\phi_y} = 0 \tag{4.15}$$

2) As $\mathbf{m_1}(\phi)$ is tangent to the inelastic loading branch at $\phi = \phi_y$, i.e. $\frac{d\mathbf{m_1}}{d\phi} = p(EI)_e$, it follows that

$$\frac{dS_d}{d\phi}\Big|_{\phi=\phi_y} = 0 \tag{4.16}$$

3) $\mathbf{m_1} = M_f$ at $\phi = \phi_f$, i.e.

$$M_f = (\phi_f - \phi_y)p(EI)_e + M_y - A \cdot \left[\left(\frac{\phi_f}{\phi_u}\right)^{2\omega} + B\left(\frac{\phi_f}{\phi_u}\right)^{\omega} + C\right]\Delta M_f \tag{4.17}$$

Using Eqs (4.15) and (4.16), one obtains $B = -2\left(\frac{\phi_y}{\phi_u}\right)^{\omega}$, $C = \left(\frac{\phi_y}{\phi_u}\right)^{2\omega}$. Similarly, Eq (4.17) yields $A = \left(\frac{\phi_u}{\phi_f - \phi_y}\right)^{\omega}$, so that

$$S_d = \left(\frac{\phi - \phi_y}{\phi_f - \phi_y}\right)^{\omega} \tag{4.18}$$

and

$$\mathbf{m_1}(\phi) = (\phi - \phi_y)p(EI)_e + M_y - \Delta M \tag{4.19}$$

where

$$\Delta M = [(\phi_f - \phi_y)p(EI)_e + M_y - M_f]\left(\frac{\phi - \phi_y}{\phi_f - \phi_y}\right)^{\omega} \tag{4.20}$$

Using Figs. 4.9-4.12 which show the comparisons between experimental and analytical nonlinear responses, the value of free parameter, ω, can be determined to be 1.5.

In order to incorporate this concept of strength deterioration into the hysteresis model, an imaginary point with coordinates $(\overline{\phi}_x, \overline{M}_x)$, is introduced, at which the load-deformation curve is aimed during reloading(see Fig. 4.3), such that

$$\frac{\overline{M}_x - M_y}{\overline{\phi}_x - \phi_y} = p(EI)_e \tag{4.21}$$

and the effective stiffness during reloading becomes

$$(\overline{EI}) = \frac{M'_x - M_o^-}{\phi_x - \phi_o^-} = \frac{\overline{M}_x - M_o^-}{\overline{\phi}_x - \phi_o^-} \tag{4.22}$$

where (ϕ_x, M_x) is the point of maximum previous loading. The actual strength M'_x, reached at curvature ϕ_x, follows from Eq (4.19),

$$M'_x = M_x - \Delta M \tag{4.23}$$

Then, using Eqs (4.21) and (4.22), the coordinates of the imaginary point become

$$\overline{\phi}_x = \frac{1}{(\overline{EI}) - p(EI)_e}\left[M_y - M_o^- - \phi_y p(EI)_e + \phi_o^-(\overline{EI})\right] \tag{4.24}$$

$$\overline{M}_x = M_o^- + \frac{(\overline{EI})}{(\overline{EI}) - p(EI)_e}\left[M_y - M_o^- + (\phi_o^- - \phi_y)p(EI)_e\right] \tag{4.25}$$

4.3 Shear Effect on Hysteretic Behaviour

The effect of shear has been investigated by many researchers(1,10,15,21,23,31). When load reversal occurs within the inelastic range in the presence of high shear, the open shear cracks will initially permit the transfer of shear forces mostly through dowel action only, leading to a rather low stiffness. After the closing of such cracks, aggregate interlock and shear friction cause a significant increase of the member stiffness. Roufaiel(31) has modeled this effect by introducing the "crack-closing" moment M_p, associated with curvature ϕ_p, Fig. 4.4. The point (M_p^+, ϕ_p^+), can be determined as follows. If shear stresses are negligible and the hysteresis loops are stable during cyclic loading, no pinching is likely to occur and branches 4 and 5 will form a single straight line. In this case, the point (M_p^+, ϕ_p^+), will degenerate to a "point of no pinching", with the following coordinates (Fig. 4.4):

$$\phi_n^+ = \phi_r^- \frac{(\overline{EI})}{(\overline{EI}) - (EI)_e} \tag{4.26}$$

$$M_n^+ = (EI)_e \phi_n^+ \tag{4.27}$$

where

$$(\overline{EI}) = \frac{\overline{M}_x}{\overline{\phi}_x - \phi_r} \tag{4.28}$$

A "pinching factor" α_p, is now introduced such that $\alpha_p = 1$, if the shear effect is negligible, and $\alpha_p = 0$, if the shear effect completely controls the load-deformation behaviour.

The coordinates of the crack-closing point can then be expressed as:

$$M_p^+ = \alpha_p M_n^+ \tag{4.29}$$

$$\phi_p^+ = \alpha_p \phi_n^+ \tag{4.30}$$

where

$$\alpha_p = \begin{cases} 0 & \text{if} \quad \frac{a}{d} \leq 1.5 \\ 0.4\frac{a}{d} - 0.6 & \text{if} \quad 1.5 < \frac{a}{d} \leq 4.0 \\ 1 & \text{if} \quad \frac{a}{d} > 4.0 \end{cases}$$

$\frac{a}{d}$: shear span ratio, $\quad a = \frac{l}{2}$ in general

4.4 Definition of Failure

For RC members undergoing cyclic loading, several investigators have defined failure as the point where the member strength(moment) at maximum displacement (curvature) has dropped below 75% of the initial yield strength(moment). But if the member is subsequently loaded beyond this maximum displacement or curvature, its moment can be observed to increase well above the 75% level(15,16), even though it has assumed to be already "failed"(see Fig. 2.1). For this reason it is necessary to relate the failure definition to the actual strength reserve or residual strength, which is a function of the experienced loading history.

First, the failure curvature ϕ_f for monotonic loading needs to be defined. It depends on a number of different variables such as concrete strength, confinement

ratio, and axial force, which in turn determine the failure mode. A section may fail in flexure due to concrete crushing or fracture of the tensile steel, or it may fail because the compression steel buckles. Other failure modes are related to shear or bond failures. Given the complete stress-strain curves for steel and concrete, and the cross-sectional dimensions, it is possible to compute the failure curvature for monotonic loading(see Appendix A).

In order to relate the failure moment at some arbitrary curvature ϕ_i to the actually experienced load history, it is necessary to refer to the strength drop due to one load cycle, which was introduced in Section 4.2. If the total strength drop down to the failure moment M_{fi} at some curvature ϕ_i is known, the number of cycles to this curvature level needed to cause failure, can be determined(Fig. 4.5).

The failure moments for different curvature levels are plotted in the failure curve of Fig. 4.5,

$$M_{fi} = M_f \cdot \frac{2\Phi_i}{\Phi_i + 1.0} \tag{4.31}$$

where

M_{fi} : failure moment for given curvature level ϕ_i

M_f : failure moment for monotonic loading

$\Phi_i = \frac{\phi_i}{\phi_f}$: curvature ratio

ϕ_f : failure curvature for monotonic loading

According to Fig. 4.5, the failure moment M_{fi} decreases with smaller curvature levels ϕ_i, i.e. larger strength drops from the monotonic loading curve are needed to lead to failure. As can be seen, a simple definition of $M_{fi} = 0.75M_y$ is not very meaningful.

4.5 A New Damage Index and Damage Accelerator

Based on the above definition of failure, we shall now propose a new damage model as a rational measure of damage sustained by RC members undergoing strong cyclic loading. It is again emphasized that damage increments are proportional to the amount of dissipated energy and displacement or curvature level.

The proposed damage index D_e combines a modified Miner's hypothesis with damage acceleration factors, which reflect the effect of the loading history, and it considers the fact that RC members typically respond differently to positive and negative moments:

$$D_e = \sum_i \sum_j \left(\alpha_{ij}^{+} \frac{n_{ij}^{+}}{N_i^{+}} + \alpha_{ij}^{-} \frac{n_{ij}^{-}}{N_i^{-}} \right) \tag{4.32}$$

where

i : indicator of different displacement or curvature levels

j : indicator of cycle number for a given load level i

$N_i = \dfrac{M_i - M_{fi}}{\Delta M_i}$: number of cycles(with curvature level i) to cause failure

n_{ij} : number of cycles(with curvature level i) actually applied

α_{ij} : damage accelerator

$+, -$: indicator of loading sense

When counting load cycles, n_{ij}, only those cycles are considered, which enter the shaded area shown in Fig. 4.6, i.e. load cycles (1) and (2) are not counted when computing the damage index D_e. This can be justified on the grounds that load cycle (1) can hardly incur damage during the closing of existing cracks, whereas load cycle (2) can cause only a negligible amount of damage.

The loading history effect is captured by including the damage accelerator α_{ij},

which, for positive moment loading, is defined as

$$\alpha_{ij}^{+} = \frac{k_{ij}^{+}}{\overline{k_i}^{+}} \cdot \frac{\phi_i^{+} + \phi_{i-1}^{+}}{2\phi_i^{+}} = \frac{M_{ij}^{+}}{\left[M_{i1}^{+} - \frac{(N_i^{+}-1)\Delta M_i^{+}}{2}\right]} \cdot \frac{\phi_i^{+} + \phi_{i-1}^{+}}{2\phi_i^{+}} \tag{4.33}$$

where

$$k_{ij}^{+} = \frac{M_{ij}^{+}}{\phi_i^{+}} \tag{4.34}$$

is the stiffness during the j-th cycle up to load level i,

$$\overline{k_i}^{+} = \frac{1}{N_i^{+}} \sum_{j=1}^{N_i^{+}} k_{ij}^{+} \tag{4.35}$$

is the average stiffness during N_i^{+} cycles up to load level i, and

$$M_{ij}^{+} = M_{i1}^{+} - (j-1)\Delta M_i^{+} \tag{4.36}$$

is the moment reached after j cycles up to load level i, Fig. 4.7.

The definition of Eq (4.33) needs some explanation. As Fig. 4.7 illustrates, the energy that can be dissipated during a single cycle up to a given level i decreases for successive cycles. That means the damage increments also decrease. In a constant-amplitude loading sequence, the first load cycle will cause more damage than the last one; the α_{ij}-factor decreases as load cycling proceeds. This has been considered by introducing the stiffness ratio into the damage accelerator.

As an example, consider the two load histories of Fig. 2.11a and 2.11b. The expected moment-curvature responses to these different load histories are shown qualitatively in Fig. 4.8a and 4.8b, respectively. Even though the second cycle in both cases involves the same load level, the dissipated energy(and damage incurred) is different, because the damage due to the preceding load cycles is different. As Fig. 4.8 illustrates, the factor $\frac{\phi_i^{+} + \phi_{i-1}^{+}}{2\phi_i^{+}}$, is necessary to normalize the damage increments in the case of changing load amplitudes. Thus, if the same moment level were

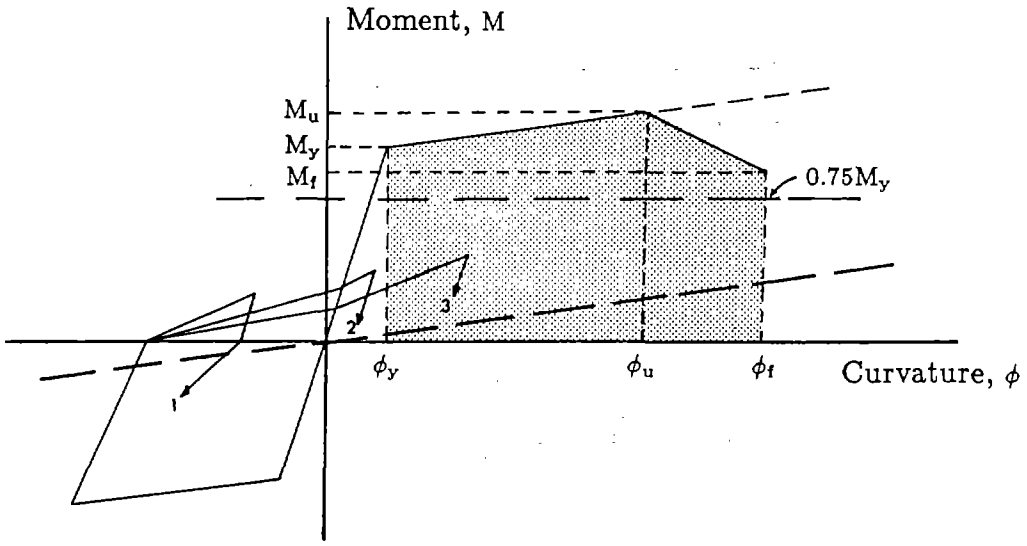

Fig. 4.6 - Domain for damaging load of positive sense

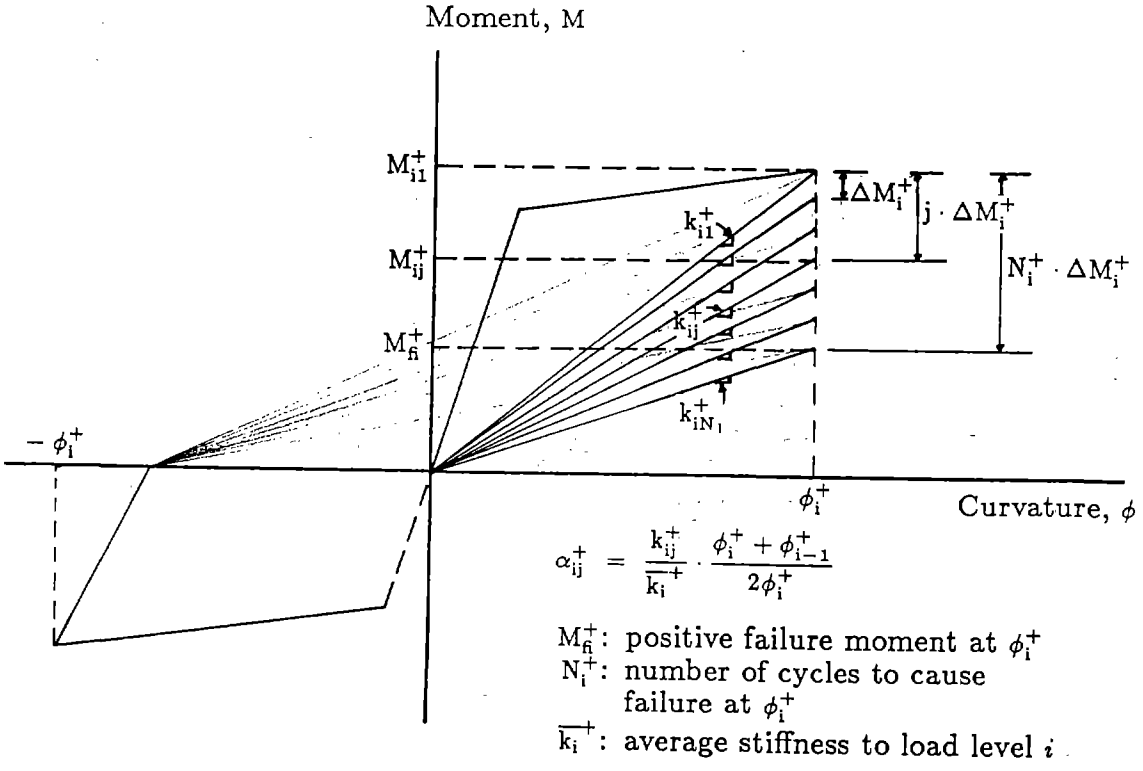

Fig. 4.7 - Definition of positive damage accelerator

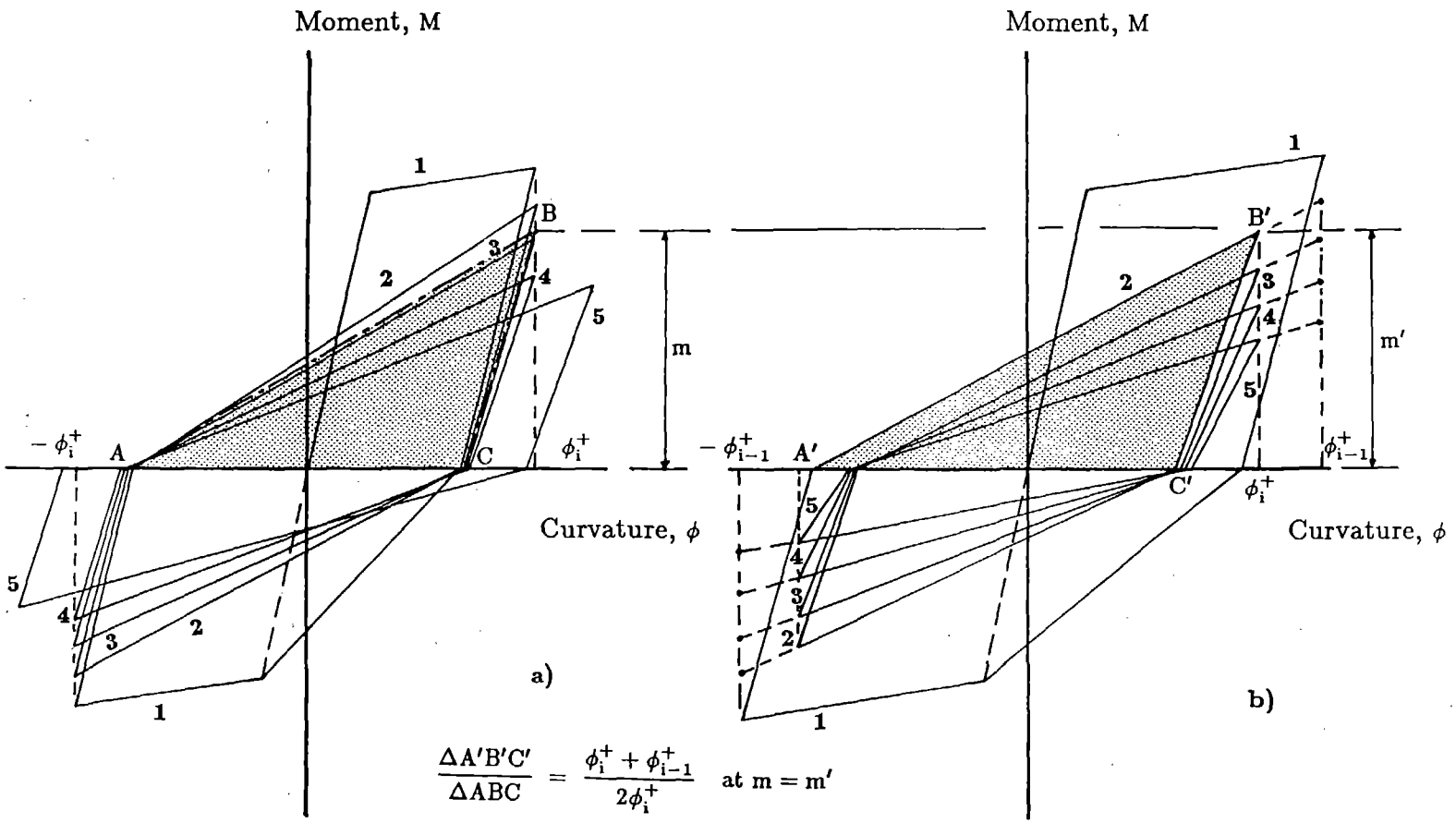

Fig. 4.8 - Definition of coeffcients for damage accelerator

reached in the two cases depicted, the damage accelerator would still be the same, even though the dissipated energies are not.

For negative loading, the damage accelerator is defined similarly,

$$\alpha_{ij}^{-} = \frac{k_{ij}^{-}}{\overline{k_i}^{-}} \cdot \frac{\phi_i^{-} + \phi_{i-1}^{-}}{2\phi_i^{-}} = \frac{M_{ij}^{-}}{\left[M_{i1}^{-} - \frac{(N_i^{-}-1)\Delta M_i^{-}}{2}\right]} \cdot \frac{\phi_i^{-} + \phi_{i-1}^{-}}{2\phi_i^{-}} \tag{4.37}$$

$$k_{ij}^{-} = \frac{M_{ij}^{-}}{\phi_i^{-}} \tag{4.38}$$

$$\overline{k_i}^{-} = \frac{1}{N_i^{-}} \sum_{j=1}^{N_i^{-}} k_{ij}^{+} \tag{4.39}$$

$$M_{ij}^{-} = M_{i1}^{-} - (j-1)\Delta M_i^{-} \tag{4.40}$$

In order to illustrate the capabilities of the proposed mathematical model, four quasi-static experimental load-deformation curves have been simulated numerically. As the comparisons between experimental and analytical responses in Figs. 4.9-4.12 suggest, the reproduction of hysteretic behaviour of RC members appears to be sufficiently accurate. Therefore, the new model can serve as a reliable tool for predicting earthquake induced damage in RC members. However, because of the shortage of pertinent low cycle fatigue experimental data, the calibration of some of the free model parameters cannot be considered final.

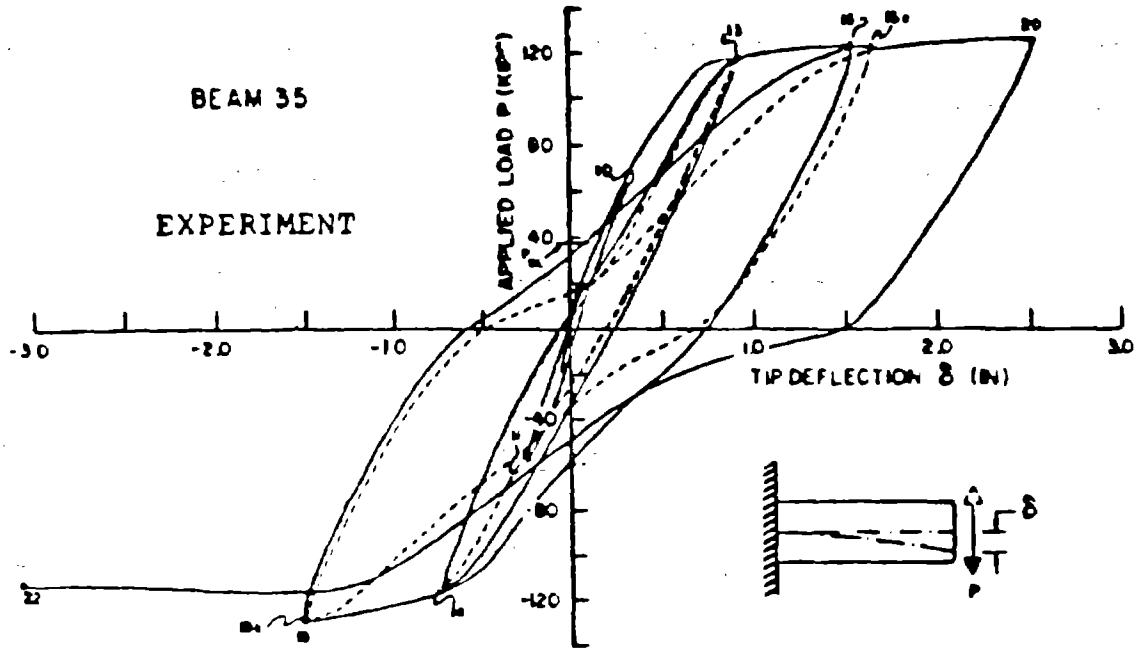

a) Experiment

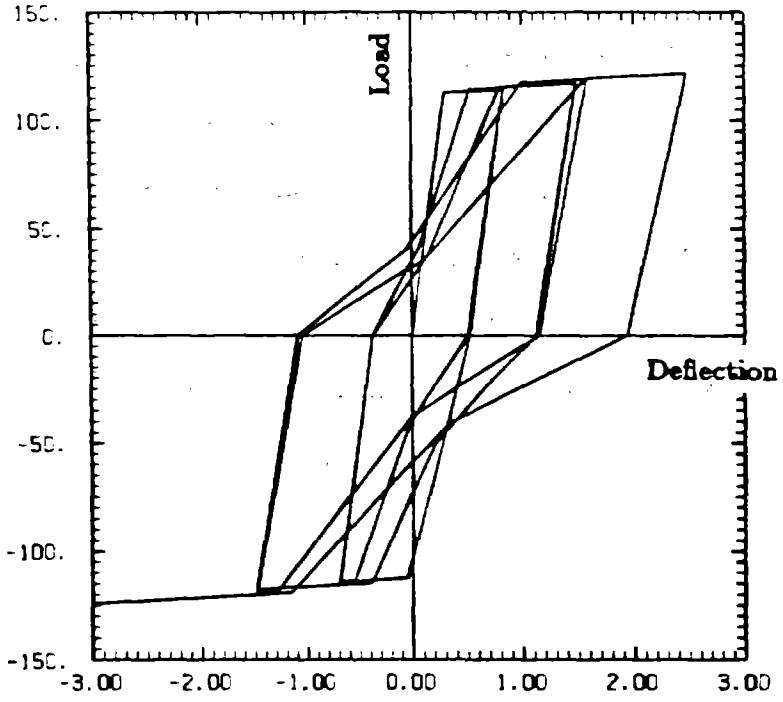

b) Analysis

Fig. 4.9 - Experimental and analytic load-deformation curves for beam B35 tested by Popov, Bertero and Krawinkler(Ref. 57)

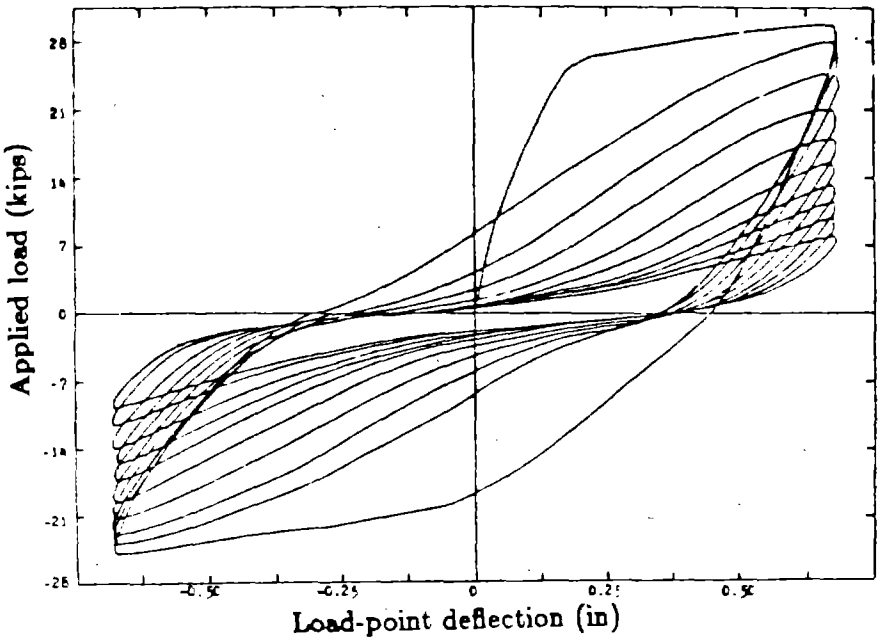

a) Experiment

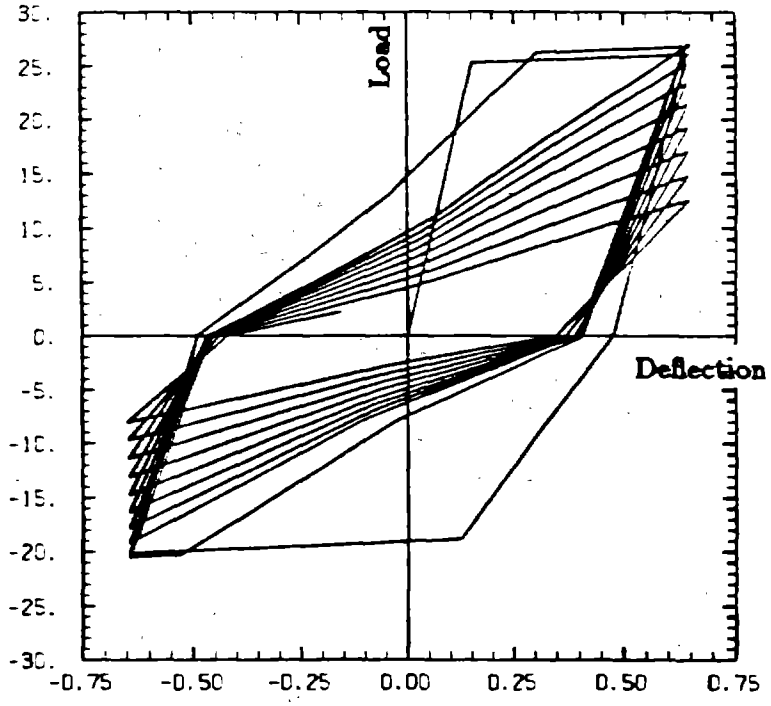

b) Analysis

Fig. 4.10 - Experimental and analytic load-deformation curves for beam S2-2 tested by Hwang(Ref. 15)

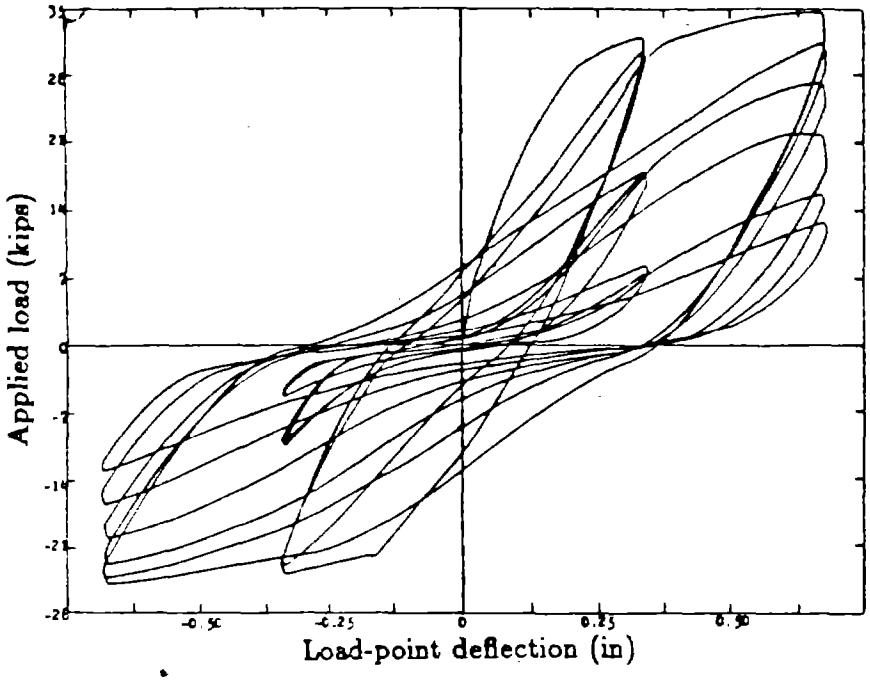

a) Experiment

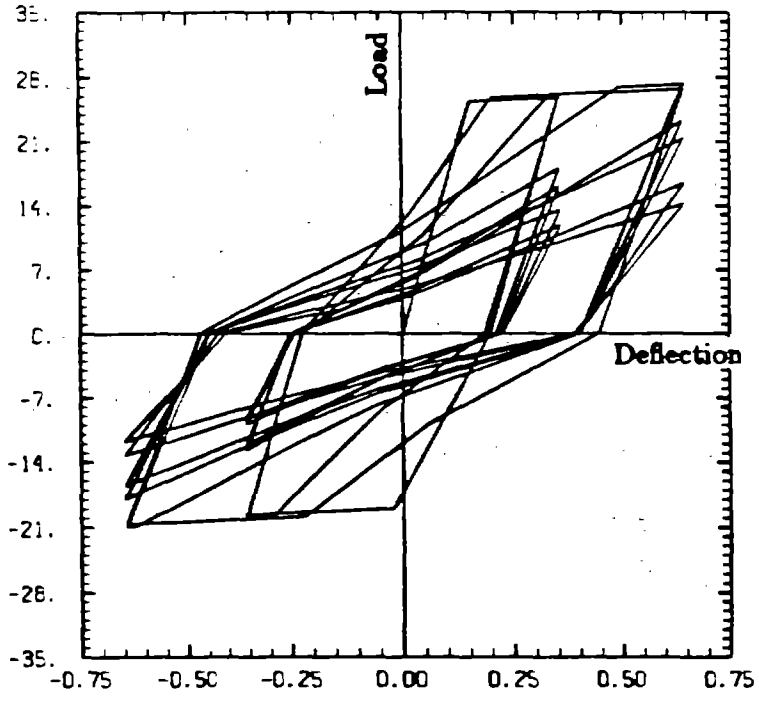

b) Analysis

Fig. 4.11 - Experimental and analytic load-deformation curves for beam S2-3 tested by Hwang(Ref. 15)

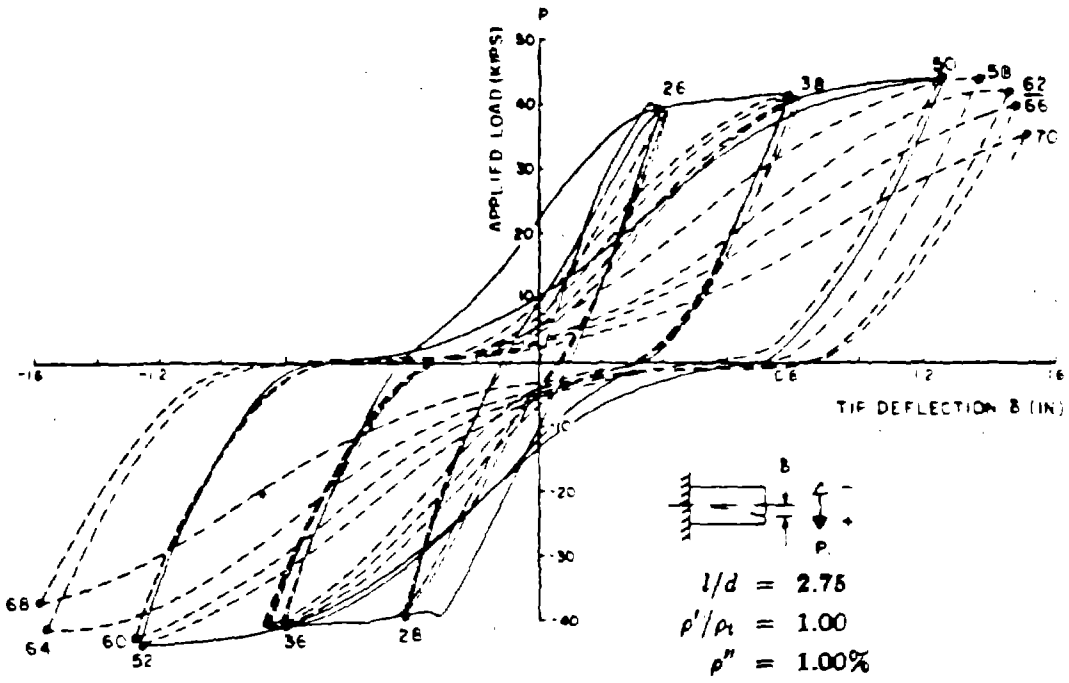

a) Experiment

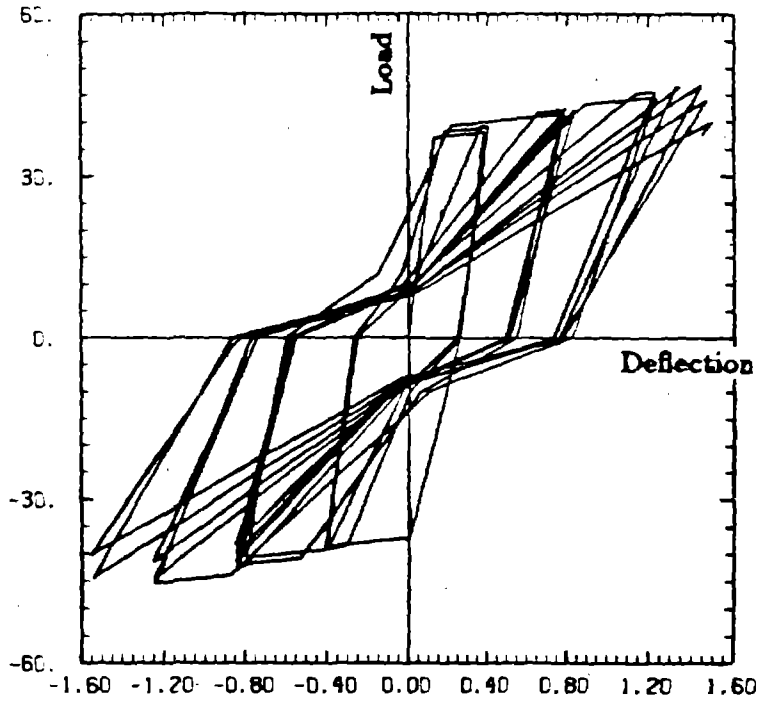

b) Analysis

Fig. 4.12 - Experimental and analytic load-deformation curves for beam R5 tested by Ma, Bertero and Popov(Ref. 21)

5. Conclusions and Recommendations for Future Study

In this report, a number of previously proposed damage models for reinforced concrete members have been reviewed. The more recent models assume that damage is a linear combination of high load levels and the energy dissipated during inelastic load cycles.

A new damage model has been proposed herein, which is believed to be more rational and which takes factors into account(such as the loading sequence), which are ignored in the other models. It is based on a thorough study of the many factors that can contribute to damage of reinforced concrete members. A number of parameters were calibrated against the few available experimental results. For example, the rate of strength deterioration and damage accelerating factors were thus determined.

An accurate determination of damage is essential for meaningful nonlinear dynamic analysis of concrete structures, because the damage index is closely tied to the residual strength reserve of a member, after it has undergone large inelastic load cycles.

The principal shortcoming of the model is the small number of test data on which it is based. Thus, it is important that experimental investigations be undertaken, with the following objectives:

1) to determine a clear relationship between load(deformation) level and energy dissipation capacity(as shown schematically in Fig. 2.13);
2) to substantiate the modified Miner's rule for varying load amplitudes;
3) to verify the damage accelerators of Eq (4.33);
4) to verify the strength deterioration curve of Fig. 4.4;
5) to verify the failure definition curve of Fig. 4.5;
6) to study the influence of important parameters, such as confinement ratio,

longitudinal steel reinforcement ratio, shear reinforcement, etc.

Once the damage model has been thoroughly verified, it will be possible to use it in a nonlinear dynamic analysis procedure to maximum effect.

References

1) Atalay, M. B. and Penzien, J., "The Seismic Behaviour of Critical Regions of Reinforced Concrete Components as Influenced by Moment, Shear and Axial Forces," Report No. EERC-75-19, University of California, Berkeley, CA, December 1975.

2) Banon, H., Biggs, J. M. and Irvine, H. M., "Prediction of Seismic Damage in Reinforced Concrete Frames," Publication No. R80-16, Dept. of Civil Engin., MIT, Cambridge, MA, May 1980.

3) Banon, H., Biggs, J. M. and Irvine, H. M., "Seismic Damage in Reinforced Concrete Frames," Journal of the Structural Division, ASCE, Vol. 107, No. ST9, September 1981.

4) Banon, H. and Veneziano, D., "Seismic Safety of Reinforced Concrete Members and Structures," Earthquake Engineering and Structural Dynamics, Vol. 10, 1982.

5) Bertero, V. V., and Bresler, B., "Design and Engineering Decision: Failure Criteria (Limit States), Developing Methodologies for Evaluating the Earthquake Safety of Existing Buildings," Report No. EERC-77-6, University of California, Berkeley, CA, February 1977.

6) Blejwas, T., and Bresler, B., "Damageability in Existing Buildings ," Report No. EERC-78-12, University of California, Berkeley, CA, August 1979.

7) Blume, J. A., Wang, E. C. W., Scholl, R. E. and Shah, H. C., " Earthquake Damage Prediction: A Technological Assessment," Report No. 17, Dept. of Civil Engin., Stanford University, Stanford, CA, October 1975.

8) Czarnecki, R. M., "Earthquake Damage to Tall Buildings," Report No. R73-8, Dept. of Civil Engin., MIT, Cambridge, MA, January 1973.

9) Culver, C. G., Lew, H. S., Hart, G. C., and Pinkham, C. W., "Natural Hazards Evaluation of Existing Building," National Bureau of Standards, Building Science Series No. 61, January 1975.

10) Darwin, D. and Nmai, C. K., "Energy Dissipation in RC Beams under Cyclic

Load", Journal of Structural Engineering, ASCE, Vol. 112, No. 8, August 1986.

11) Four papers by ASCE Committee on Fatigue and Fracture Reliability, Journal of the Structural Division, ASCE, January 1982.

12) Earthquake Engineering Systems, "A Rational Approach to Damage Mitigation in Existing Structures Exposed to Earthquakes," Earthquake Engineering Systems, Inc., San Francisco, CA, May 1978.

13) Gosain, N. K., Brown, R. H. and Jirsa, J. O., "Shear Requirements for Load Reversals on RC Members," Journal of the Structural Division, ASCE, Vol. 103, No. ST7, July 1977.

14) Hafen, D. and Kintzer, F. C., "Correlations Between Ground Motion and Building Damage Engineering Intensity Scale Applied to the San Fernando Earthquake of February 1971," Report No. JAB-99-111, John A. Blume and Associates, Engineers, San Franscisco, CA, November 1977.

15) Hwang, T. H., " Effects of Variation in Load History on Cyclic Response of Concrete Flexural Members," Ph.D. Thesis, Dept. of Civil Engin., University of Illinois, Urbana, IL, 1982.

16) Hwang, T. H. and Scribner C. F., "R/C Member Cyclic Response During Various Loadings," Journal of Structural Engineering, ASCE, Vol. 110, No. 3, March 1984.

17) Kasiraj, I. and Yao, J. T. P., "Fatigue Damage in Seismic Structures," Journal of the Structural Division, ASCE, Vol. 95, No. ST8, August 1969.

18) Krawinkler, H. and Zohrei, M., "Cumulative Damage in Steel Structures Subjected to Earthquake Ground Motions," Computers and Structures, Vol. 16, No. 14, 1983.

19) Lee, D. L. N., Hanson, R. D., and Wight, J. K., "Original and Repaired Reinforced Concrete Beam-Column Subassemblages Subjected to Earthquake Type Loading," Report No. UMEE 76R4, University of Michigan, Ann Arbor, MI, April 1976.

20) Lybas, J. and Sozen, M. A., "Effect of Beam Strength and Stiffness on Dynamic Behaviour of Reinforced Concrete Coupled Walls," Civil Engineering Studies, SRS No. 444, University of Illinois, Urbana, IL, July 1977.

21) Ma, S-Y. M., Bertero, V. V. and Popov, E. P., "Experimental and Analytical Studies on the Hysteretic Behaviour of Reinforced Concrete Rectangular and T-Beams," Report No. EERC-76-2, University of California, Berkeley, CA, May 1976.

22) Mindess, S. and Young, J. T., "Concrete," Prentice-Hall,Inc., Englewood Cliffs, 1981.

23) Nmai, C. K. and Darwin, D., "Lightly Reinforced Concrete Beams under Cyclic Load", ACI Journal, Title No. 83-72, September-October 1986.

24) Oliveira, C. S., "Seismic Risk Analysis for a Site and a Metropolitan Area," Report No. EERC-75-3, University of California, Berkeley, CA, August 1975.

25) Park, Y. J., Ang, A. H-S. and Wen, Y. K., "Seismic Damage Analysis and Damage-Limiting Design of R/C Structures," Journal of Structural Engineering, ASCE, Vol. 113, No. 4, April 1985.

26) Park, Y. J., Ang, A. H-S. and Wen, Y. K., "A Mechanistic Seismic Damage Model for Reinforced Concrete," Journal of Structural Engineering, ASCE, Vol. 111, No. 4, April 1985.

27) Park, Y. J., "Seismic Damage Analysis and Damage-Limiting Design of R/C Structures," Ph.D. Thesis, Dept. of Civil Engin., University of Illinois, Urbana, IL, 1984.

28) Park, R. and Paulay, T., "Reinforced Concrete Structures," John Wiley and Sons, Inc, New York, NY, 1975.

29) Rolfe, S. T. and Barsom, J. M., "Fracture and Fatigue Control in Structures," Prentice-Hall, Inc, Englewood Cliffs, 1977.

30) Rolfe, S. T., "Fracture and Fatigue Control in Steel Structures," Engineering Journal, AISC, January 1977.

31) Roufaiel, M. S. L. and Meyer, C., "Analysis of Damaged Concrete Frame Build-

ings," Report No. NSF-CEE81-21359-1, Dept. of Civil Engin. and Engin. Mech., Columbia University, New York, NY, 1983.

32) Roufaiel, M. S. L. and Meyer, C., "Reliability of Concrete Frames Damaged by Earthquakes," Journal of Structural Engineering, ASCE, Vol. 113, No. 3, March 1987.

33) Roufaiel, M. S. L. and Meyer, C., "Analytical Modeling of Hysteretic Behaviour of R/C Frames," Journal of Structural Engineering, ASCE, Vol. 113, No. 3, March 1987.

34) Sauter, F. F., "Damage Prediction for Earthquake Insurance," San Jose, Costa Rica, 1979.

35) Schickert, G. and Danssmann, J., "Behaviour of Concrete Stressed by High Hydrostatic Compression," International Conference on Concrete under Multiaxial Conditions, Toulouse, May 22-24, 1984.

36) Scribner, C. F. and Wight, J. K., "Delaying Shear Strength Decay in Reinforced Concrete Flexural Members under Large Load Reversals," Report No. UMEE 78R2, Dept. of Civil Engin., University of Michigan, Ann Arbor, May 1978.

37) Seed, H. B., Idriss, I. M. and Dezfulian H., "Relationships Between Soil Conditions and Building Damage in the Caracas Earthquake of July 29, 1967," Report No. EERC-70-2, University of California, Berkeley, CA, February 1970.

38) Sinha, B. P., Gerstle, K. H., and Tulin, L. G., "Stress-Strain Relations for Concrete under Cyclic Loadings," ACI Journal, February 1964.

39) Stephens, J. E. and Yao, J. T. P., "Damage Assessment Using Response Measurement," Journal of Structural Engineering, ASCE, Vol. 113, No. 4, April 1987.

40) Tang, J. P. and Yao, J. T. P., "Expected Fatigue Damage of Seismic Structures," Journal of the Engineering Mechanics Division, ASCE, Vol. 98, No. EM3, June 1972.

41) URS/Blume, J. A. and Associates, "Effects Prediction Guidelines for Structures Subjected to Ground Motion," San Francisco, CA, 1975.

42) Whitman, R. V., Cornell, C. A., Vanmarcke, E.H. and Reed, J.W., "Methodology and Initial Damage Statistics," Report R73-57, No. ST380, Dept. of Civil Engin., MIT, Cambridge, MA, 1972.

43) Whitman, R. V., Hong, J. T. and Reed, J. W., "Damage Statistics for High Rise Buildings in the Vicinity of the San Fernando Earthquake," Report R73-24, Seismic Design Analysis Report No.7, MIT, Cambridge, MA, 1973.

44) Whitman, R. V. and Biggs, J. M., "Seismic Design Decision Analysis - Methodology and Pilot Application," Report No. 10, Structures Publication No. 385, MIT, Cambridge, MA, 1974.

45) Wiggins, J. H., Jr. and Moran, D. V., "Earthquake Safety in the City of Long Beach Based on the Concept of Balanced Risk," J.H. Wiggins Company, Redondo Beach, CA, September 1971.

46) Wight, J. K. and Sozen, M. A., "Shear Strength Decay in Reinforced Concrete Columns Subjected to Large Deflection Reversals," Civil Engineering Studies, SRS No. 4-3, University of Illinois, Urbana, IL, August 1973.

47) Wong, E. H. and Whitman R. V., "Correlations Between Earthquake Damage and Strong Ground Motion," Report No. R75-23, Dept. of Civil Engin., MIT, Cambridge, MA, June 1975.

48) Yao, J. T. P., and Munse, W. H., "Low-Cycle Axial Fatigue Behaviour of Mild Steel," Journal of the Structural Division, ASCE, Vol. 95, No. ST8, August 1969.

49) Nishigaki, T. and Mizuhata, K., "Experimental Study on Low-Cycle Fatigue of Reinforced Concrete Columns," Report No. 328, Journal of Japanese Architectural Society, Japan, June, 1983.

50) Nishigaki, T. and Mizuhata, K., "Evaluation of Seismic Safety for Reinforced Concrete Structures," Report No. 332, Journal of Japanese Architectural Society , October, 1983.

51) Mizuhata, K., "Evaluation of Seismic Safety for Reinforced Concrete Structures due to Low-Cycle Fatigue," Report No. GBRC Vol.10 No.4, Laboratory of

Japanese Architectural Society, Japan, 1985.

52) Mizuhata, K., Sugiyama, K. and Shimizu H., "Comparative Study on the Evaluation Method of Cumulative Damage of Reinforced Concrete Columns," Report in the Kinki-Division of Japanese Architectural Society, Japan, 1987.

53) Chan, W. W. L., "The Ultimate Strength and Deformation of Plastic Hinges in Reinforced Concrete Frameworks," Magazine of Concrete Research, Vol. 7, No. 21, November 1955.

54) Soliman, M. T. M. and Yu, C. W., "The Flexural Stress-Strain Relationship of Concrete Confined by Rectangular Transverse Reinforcement," Magazine of Concrete Research, Vol. 19, No. 61, December 1967.

55) Roy, H. E. H. and Sozen, M. A., "Ductility of Concrete," Proceedings of the International Symposium on Flexural Mechanics of Reinforced Concrete, ASCE-ACI, Miami, November 1964.

56) Kent, D. C. and Park, R., "Flexural Members with Confined Concrete," Journal of the Structural Division, ASCE, Vol. 97, ST7, July 1971.

57) Popov, E. P., Bertero, V.V. and Krawinkler, H., "Cyclic Behaviour of Three RC Flexural Members with High Shear," Report No. EERC-72-5, University of California, Berkeley, October, 1972.

Appendix A - Primary Moment-Curvature Relationship

Herein, an analytical primary moment-curvature relationship will be derived for a section, which includes a new definition of failure. Among the various possible failure modes, also that of buckling of the compression reinforcement is included.

A.1 Material Constitutive Laws

A.1.1 Concrete

It is well known that concrete has different behaviour in tension and compression. The tensile strength can be ignored under seismic loading, because much of it is lost due to cracks caused by service loads. The stress-strain curve for plain concrete has been idealized by many researchers.(53,54,55,56) Herein, Roufaiel and Meyer's trilinear curve(31) has been adopted, with some minor modifications, Fig. A.1. It is fully described by specifying the following parameters,

$$f_{cu} = \alpha_c f'_c \,, \quad f_{cy} = \frac{3}{4} f_{cu} \,, \quad \epsilon_{cu} = \alpha_c \epsilon_o \,, \quad \epsilon_{cy} = \frac{5}{12} \epsilon_{cu} \,, \quad \epsilon_{cm} = \beta_c \epsilon_{cu} \qquad (A.1)$$

where f'_c is the uniaxial strength of concrete, ϵ_o is the strain at f'_c, and ϵ_{cm} is the critical strain, at which the concrete cover can be observed to spall off, and which can be correlated to the onset of failure. Factors α_c and β_c reflect the confining effect of transverse steel on concrete strength and critical strain, respectively; according to (31),

$$\begin{aligned} \alpha_c &= 1 + 10\rho'' \\ \beta_c &= 2 + 600\rho'' \end{aligned} \qquad (A.2)$$

where

$$\rho'' = \frac{2\left(b'' + d''\right) A_v}{b'' \, d'' \, s} \quad : \text{volumetric confinement ratio}$$

b'', d'' : width and depth of the confined core, Fig. A.5

A_v : cross sectional area of transverse steel

s : spacing of transverse steel

The stiffnesses of the three branches of the stress-strain curve of Fig. A.1 follow as,

$$E_c = \frac{f_{cy}}{\epsilon_{cy}} = \frac{1.8\ f_{cu}}{\epsilon_{cu}}$$
$$P_c\ E_c = \frac{5}{21}\ E_c \qquad (A.3)$$
$$-\bar{P}_c E_c = \frac{f_{cu}\ -\ 0.1 f'_c}{\epsilon_{cu} - \epsilon_{cm}}$$

A.1.2 Tensile Reinforcing Steel

The stress-strain curves for steel bars are often idealized by bilinear curves, Fig. A.2, characterized by Young's modulus,

$$E_s = \frac{f_{sy}}{\epsilon_{sy}} \qquad (A.4)$$

for the elastic part, and by the strain hardening parameter,

$$P_s = \frac{1}{E_s} \cdot \frac{f_{su} - f_{sy}}{\epsilon_{su} - \epsilon_{sy}} \qquad (A.5)$$

for the inelastic part, where

f_{sy} : yield stress

f_{su} : ultimate stress

ϵ_{sy} : yield strain

ϵ_{su} : ultimate strain

and

$$-\bar{P}_c E_c = \gamma P_c E_c \qquad (A.6)$$

for the unloading part, where γ can be determined from experimental test data for reinforcing steels. In this analysis, $\gamma = 2.0$ is used.

The descending branch of the steel stress-strain curve has significance only for the material point undergoing failure. In a real reinforcing bar, strain localization

leads to failure as soon as $\epsilon_s = \epsilon_{su}$ is reached. However, in order to facilitate our strength-drop model, it is assumed that failure is only initiated at the strain ϵ_{su} and completed when $\epsilon_s = \alpha\epsilon_{su}$. In this analysis, $\alpha = 1.5$. In an actual response analysis, a steel strain $\epsilon_s = \epsilon_{su}$ will automatically be interpreted as complete failure.

A.1.3 Compressive Reinforcing Steel

The stress-strain curve for steel in compression is very similar to that in tension, provided buckling is prevented. In the light of this restriction it is very rare that steel components in compression enter the strain hardening range. In reinforced concrete members, compression bars are restrained against buckling, as long as the concrete cover has not spalled off. The accurate determination of the buckling stress of compression bars is very difficult. Herein, it is assumed that the bars cannot buckle before they are strained to the point at which the concrete cover spalls off, i.e. when $\epsilon_f = \epsilon_{cm}$, Fig. A.3.

A.2 Primary Moment-Curvature Relationship

The primary moment-curvature curve relates moments to curvatures for monotonic loading. It can be idealized by three linear branches, Fig. A.4, one for the elastic loading part, one for the inelastic(strain hardening) loading part, and one for the unloading part. Once the stress-strain laws for steel and concrete are specified and the cross-sectional dimensions are known, it is relatively straightforward to compute the moment associated with any specified curvature, as will be shown below. This is in particular true for the yield moment, M_y, defined to be the moment at which the steel strain reaches the yield value ϵ_{sy}. The ultimate or maximum moment, M_u, and the failure curvature, ϕ_f, depend on the controlling failure mode.

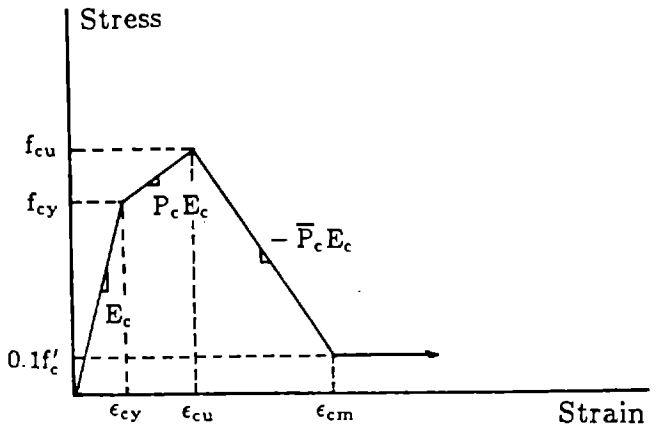

Fig. A.1 - Idealized stress-strain curve of concrete

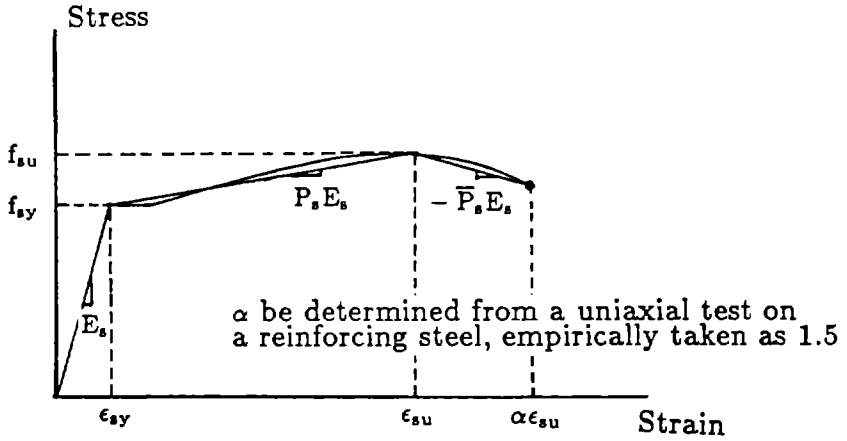

Fig. A.2 - Idealized stress-strain curve of tensile steel

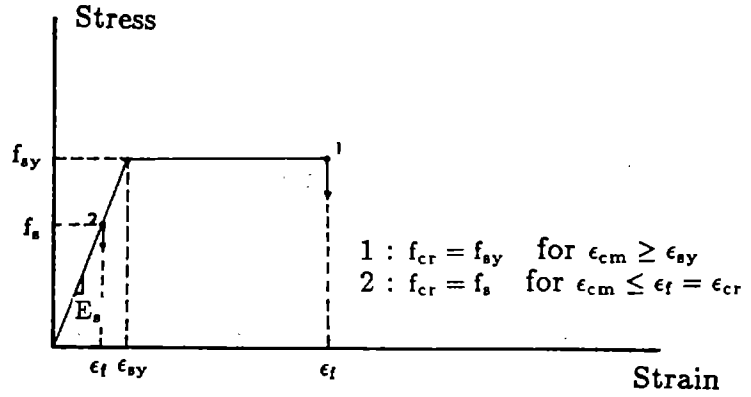

Fig. A.3 - Idealized stress-strain curve of compressive steel

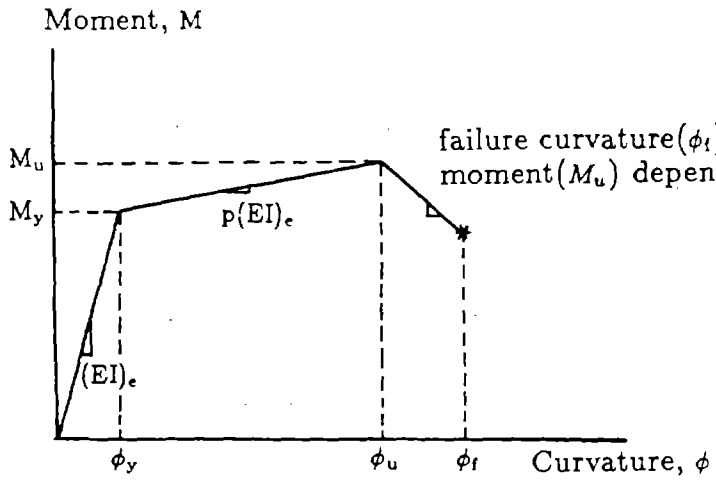

Fig. A.4 - Primary moment-curvature curve

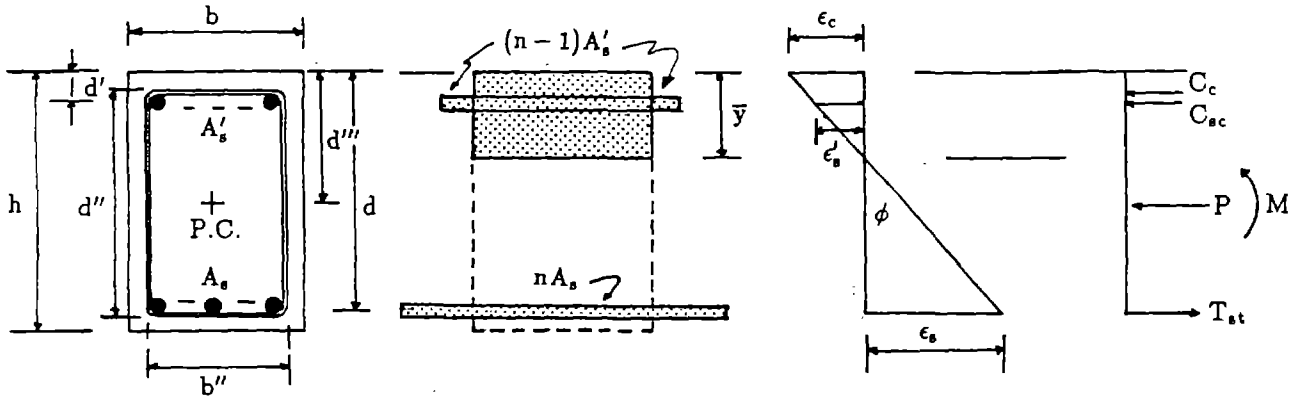

Fig. A.5 - Typical configuration of stresses and forces for reinforced concrete section

A.2.1 Neutral Axis and Curvature

To compute the neutral axis position for a given moment or curvature, the concrete strain or the tensile steel strain has to be assumed first. The complete $M - \phi$ curve can be obtained by repeatedly computing the neutral axis, $\bar{y}$, the curvature, ϕ and the bending moment, M, by increasing the concrete strain ϵ_c, or steel strain ϵ_s, from zero until any one of the possible failure modes is reached. This analysis is based on the following assumptions:

1) The stress-strain curves of reinforcing steel and concrete are idealized as shown in Fig. A.1-A.3;
2) The tensile strength of concrete is ignored;
3) Plane sections remain plane after deformation;
4) The axial force, if any, is acting at the plastic centroid of the section.

Equilibrium of all axial forces acting on the cross section shown in Fig. A.5 requires that

$$C_c + C_{s_c} - T_{s_t} - P = 0 \tag{A.7}$$

where C_c = compression force in concrete, C_{sc} = force in compression steel, T_{st} = force in the tensile steel, P = external axial force. All of these quantities can be expressed in terms of $\bar{y}$, which is the distance from the compression face to the neutral axis.

$$\alpha\bar{y}^2 + \beta\bar{y} - \gamma = 0 \tag{A.8}$$

Solving for $\bar{y}$,

$$\bar{y} = \frac{-\beta + \sqrt{\beta^2 + 4\alpha\gamma}}{2\alpha} \tag{A.9}$$

where

$$\begin{aligned} \alpha &= \alpha_c + \alpha_{s_c} + \alpha_{s_t} + \alpha_p \\ \beta &= \beta_c + \beta_{s_c} + \beta_{s_t} + \beta_p \\ \gamma &= \gamma_c + \gamma_{s_c} + \gamma_{s_t} + \gamma_p \end{aligned} \tag{A.10}$$

In the above equations, the subscripts c, s_c, s_t and p denote the contributions of concrete, compressive steel, tensile steel and axial force, respectively.

The individual terms in Eq (A.10) are tabulated in Table A.1.a-A.4.b as functions of ϵ_c or ϵ_s. The correct location of the neutral axis can be computed by iteration. Then the curvature follows as;

$$\phi = \frac{\epsilon_c}{\bar{y}} = \frac{\epsilon_s}{d - \bar{y}} \tag{A.11}$$

and the strains of interest, in terms of curvature, are

$$\begin{cases} \epsilon_s = \phi(d - \bar{y}) \\ \epsilon'_s = \phi(\bar{y} - d') \end{cases} \quad or \quad \begin{cases} \epsilon_c = \phi\bar{y} \\ \epsilon'_s = \phi(\bar{y} - d') \end{cases} \tag{A.12}$$

If the computed strains, ϵ_s(or ϵ_c) and ϵ'_s, agree with the values initially assumed, then the computed value of $\bar{y}$ is correct. Otherwise, it has to be recomputed.

A.2.2 Bending Moment

Once the correct location of $\bar{y}$ is known, moment equilibrium of all forces acting on the cross section can be established with respect to the plastic centroid, which leads to the total moment acting on the section,

$$M = M_c + M_{s_c} + M_{s_t} \tag{A.13}$$

The contribution of the concrete to the moment is

$$M_c = \begin{cases} M_{c1} & \text{for } \epsilon_c \leq \epsilon_{cy} \\ M_{c1} - M_{c2} & \text{for } \epsilon_{cy} < \epsilon_c \leq \epsilon_{cu} \\ M_{c1} - M_{c2} - M_{c3} & \text{for } \epsilon_{cu} < \epsilon_c \leq \epsilon_{cm} \\ M_{c1} - M_{c2} - M_{c3} + M_{c4} & \text{for } \epsilon_c < \epsilon_{cm} \end{cases} \tag{A.14}$$

where

$$\begin{aligned} M_{c1} &= 0.5bE_c\bar{y}^2\phi(d'' - \frac{\bar{y}}{3}) \\ M_{c2} &= 0.5bE_c\phi(1 - p_c)(\frac{\epsilon_c - \epsilon_{cy}}{\phi})^2(d'' - \frac{\epsilon_c - \epsilon_{cy}}{3\phi}) \\ M_{c3} &= 0.5bE_c\phi(p_c + \bar{p}_c)(\frac{\epsilon_c - \epsilon_{cu}}{\phi})^2(d'' - \frac{\epsilon_c - \epsilon_{cu}}{3\phi}) \\ M_{c4} &= 0.5bE_c\phi\bar{p}_c(\frac{\epsilon_c - \epsilon_{cm}}{\phi})^2(d'' - \frac{\epsilon_c - \epsilon_{cm}}{3\phi}) \end{aligned} \tag{A.15}$$

Table A.1.a - Coefficients for concrete contribution to the N.A. equation(A.7-A.9) in terms of ϵ_c

ϵ_c	α_c	β_c	γ_c
$\leq \epsilon_{cy}$	$\frac{1}{2}B$	0.0	0.0
$\epsilon_{cy} \leq \epsilon_{cu}$	$\frac{1}{2}B[1-(1-P_c)(1-\frac{\epsilon_{cy}}{\epsilon_c})^2]$	0.0	0.0
$> \epsilon_{cu} \leq \epsilon_{cm}$	$\frac{1}{2}B[1-(1-P_c)(1-\frac{\epsilon_{cy}}{\epsilon_c})^2 - (P_c+\bar{P}_c)(1-\frac{\epsilon_{cu}}{\epsilon_c})^2]$	0.0	0.0
$> \epsilon_{cm}$	$\frac{1}{2}B[1-(1-P_c)(1-\frac{\epsilon_{cy}}{\epsilon_c})^2 - (P_c+\bar{P}_c)(1-\frac{\epsilon_{cu}}{\epsilon_c})^2 + \bar{P}_c(1-\frac{\epsilon_{cm}}{\epsilon_c})^2]$	0.0	0.0

Table A.1.b - Coefficients for concrete contribution to the N¿A. equation(A.7-A.9) in terms of ϵ_s

ϵ_c	α_c	β_c	γ_c
$\leq \epsilon_{cy}$	$\frac{1}{2}B$	0.0	0.0
$\epsilon_{cy} \leq \epsilon_{cu}$	$\frac{1}{2}B[1-(1-P_c)(1+\frac{\epsilon_{cy}}{\epsilon_s})^2]$	$Bd(1-P_c)[\frac{\epsilon_{cy}}{\epsilon_s}+(\frac{\epsilon_{cy}}{\epsilon_s})^2]$	$\frac{1}{2}B(1-P_c)(d\frac{\epsilon_{cy}}{\epsilon_s})^2$
$> \epsilon_{cu} \leq \epsilon_{cm}$	$\frac{1}{2}B[1-(1-P_c)(1+\frac{\epsilon_{cy}}{\epsilon_s})^2 - (P_c+\bar{P}_c)(1+\frac{\epsilon_{cu}}{\epsilon_s})^2]$	$Bd[(1-P_c)\{\frac{\epsilon_{cy}}{\epsilon_s}+(\frac{\epsilon_{cy}}{\epsilon_s})^2\} + (P_c+\bar{P}_c)\{\frac{\epsilon_{cu}}{\epsilon_s}+(\frac{\epsilon_{cu}}{\epsilon_s})^2\}]$	$\frac{1}{2}Bd^2[(1-P_c)(\frac{\epsilon_{cy}}{\epsilon_s})^2 + (P_c+\bar{P}_c)(\frac{\epsilon_{cu}}{\epsilon_s})^2]$
$> \epsilon_{cm}$	$\frac{1}{2}B[1-(1-P_c)(1+\frac{\epsilon_{cy}}{\epsilon_s})^2 - (P_c+\bar{P}_c)(1+\frac{\epsilon_{cu}}{\epsilon_s})^2 + \bar{P}_c(1+\frac{\epsilon_{cm}}{\epsilon_s})^2]$	$Bd[(1-P_c)\{\frac{\epsilon_{cy}}{\epsilon_s}+(\frac{\epsilon_{cy}}{\epsilon_s})^2\} + (P_c+\bar{P}_c)\{\frac{\epsilon_{cu}}{\epsilon_s}+(\frac{\epsilon_{cu}}{\epsilon_s})^2\} - \bar{P}_c\{\frac{\epsilon_{cm}}{\epsilon_s}+(\frac{\epsilon_{cm}}{\epsilon_s})^2\}]$	$\frac{1}{2}Bd^2[(1-P_c)(\frac{\epsilon_{cy}}{\epsilon_s})^2 + (P_c+\bar{P}_c)(\frac{\epsilon_{cu}}{\epsilon_s})^2 - \bar{P}_c(\frac{\epsilon_{cu}}{\epsilon_s})^2]$

Table A.2.a - Coefficients for tensile steel contribution to the N.A. equation(A.7-A.9) in terms of ϵ_c

ϵ_s	α_{s_t}	β_{s_t}	γ_{s_t}
$\leq \epsilon_{sy}$	0.0	nA_s	nA_sd
$< \epsilon_{sy}$ $\leq \epsilon_{su}$	0.0	$nA_s[1-(1-P_s)(1+\frac{\epsilon_{sy}}{\epsilon_c})]$	nA_sP_sd
$> \epsilon_{su}$	0.0	$nA_s[1-(1-P_s)(1+\frac{\epsilon_{sy}}{\epsilon_c}) -(P_s+\bar{P}_s)(1+\frac{\epsilon_{su}}{\epsilon_c})]$	$-nA_s\bar{P}_sd$

Table A.2.b - Coefficients for tensile steel contribution to the N.A. equation(A.7-A.9) in terms of ϵ_s

ϵ_s	α_{s_t}	β_{s_t}	γ_{s_t}
$\leq \epsilon_{sy}$	0.0	nA_s	nA_sd
$> \epsilon_{sy}$ $\leq \epsilon_{su}$	0.0	$nA_s[1-(1-P_s)(1-\frac{\epsilon_{sy}}{\epsilon_s})]$	$nA_sd[P_s+(1-P_s)\frac{\epsilon_{sy}}{\epsilon_s}]$
$> \epsilon_{su}$	0.0	$nA_s[1-(1-P_s)(1-\frac{\epsilon_{sy}}{\epsilon_s}) -(P_s+\bar{P}_s)(1-\frac{\epsilon_{su}}{\epsilon_s})]$	$nA_sd[-\bar{P}_s+(1-P_s)\frac{\epsilon_{sy}}{\epsilon_s} +(P_s+\bar{P}_s)\frac{\epsilon_{su}}{\epsilon_s}]$

Table A.3.a - Coefficients for compressive steel contribution to the N.A. equation(A.7-A.9) in terms of ϵ_c

ϵ_{cm}	α_{s_c}	β_{s_c}	γ_{s_c}
$\leq \epsilon_{sy}$	0.0	$(n-1)A'_s$	$(n-1)A'_s d'$
$> \epsilon_{sy}$	0.0	$(n-1)A'_s \frac{\epsilon_{sy}}{\epsilon_c}$	0.0

Table A.3.b - Coefficients for compressive steel contribution to the N.A. equation(A.7-A.9) in terms of ϵ_s

ϵ_{cm}	α_{s_c}	β_{s_c}	γ_{s_c}
$\leq \epsilon_{sy}$	0.0	$(n-1)A'_s$	$(n-1)A'_s d'$
$> \epsilon_{sy}$	0.0	$-(n-1)A'_s \frac{\epsilon_{sy}}{\epsilon_s}$	$-(n-1)A'_s \frac{\epsilon_{sy}}{\epsilon_s} d$

Table A.4.a - Coefficients for axial force contribution to the N.A. equation(A.7-A.9) in terms of ϵ_c

α_p	β_p	γ_p
0.0	$-\frac{P}{E_c \epsilon_c}$	0.0

Table A.4.b - Coefficients for axial force contribution to the N.A. equation(A.7-A.9) in terms of ϵ_s

α_p	β_p	γ_p
0.0	$\frac{P}{E_c \epsilon_s}$	$\frac{Pd}{E_c \epsilon_s}$

The contribution of the tensile steel is

$$M_{s_t} = T\ (d - d'') \tag{A.16}$$

where

$$T = \begin{cases} E_s A_s \epsilon_s & \text{for } \epsilon_s \leq \epsilon_{sy} \\ E_s A_s[(1 - p_s)\epsilon_{sy} + p_s \epsilon_s] & \text{for } \epsilon_s > \epsilon_{sy} \end{cases} \tag{A.17}$$

Finally, the contribution of the compressive steel is

$$M_{s_c} = C_{s_c}\ (d'' - d') \tag{A.18}$$

where

$$C_{s_c} = \begin{cases} (n-1)E_c A'_s \epsilon'_s & \text{for } \epsilon_{cm} \leq \epsilon_{sy} \\ (n-1)E_c A'_s \epsilon_{sy} & \text{for } \epsilon_{cm} > \epsilon_{sy} \end{cases} \tag{A.19}$$

A.3 Definition of Failure under Monotonic Loading

The definition of failure contains always an element of arbitrariness. The definition proposed herein attempts to insert some objectivity by identifying limiting strains for the steel and concrete, after the exceedance of which the moment resisting capacity of a section is clearly deteriorating rapidly. Depending on the material parameters and sectional geometry, one of several failure modes may become controlling.

1) Flexural failure due to concrete crushing

According to Fig. A.1, concrete gets crushed in compression, when the compression strain reaches the value ϵ_{cm}. For this to happen in a properly underreinforced section for a monotonically increasing load, the tension steel must first undergo a considerable amount of yielding. The numerical failure in this particular mode is easy to identify. The actual point of failure shall be defined as that curvature, for which the strength drop exceeds 25% of the yield moment, i.e. if $M \leq 0.75 M_y$.

2) Flexural failure due to fracture of tensile steel

This failure mode is assumed to lead to sudden and complete loss of strength, should the strain in the tensile reinforcement reach the value $\alpha \cdot \epsilon_{su}$(Fig. A.2), which will be determined from a uniaxial test on reinforcing steel but hereon be empirically considered as $1.5\epsilon_{su}$. For a certain unfortunate combination of design variables, it is conceivable that this might happen before the concrete strain reaches the crushing value ϵ_{cm}.

3) Flexural failure due to buckling of compression reinforcement

As was illustrated in Fig. A.3, the compression bars can buckle only after spalling of the concrete cover. Since it is rare that the concrete spalls off before the bars reach their yield strain, it is most likely that the buckling will follow immediately the spalling of the cover, whereupon the capacity of the bars to carry compression forces will drop rapidly. Herein, the bar strength is set to zero, as soon as the critical strain is reached. A rapid loss of moment capacity of the section will be the result.

4) Other failure modes

In addition to the failure modes described above, there may be others such as flexural shear failure initiated by vertical flexural cracks, web shear failure triggered by diagonal cracks or yield of vertical stirrups, failure due to loss of bond. However, these failure modes are unlikely under monotonic loading and can be avoided by following proper design procedures.

This definition of failure completes the primary moment-curvature curve for a section.